UNIVERSITÀ DEGLI STUDI DI PARMA

DIPARTIMENTO DI FARMACIA

DOTTORATO DI RICERCA IN SCIENZE DEL FARMACO, DELLE BIOMOLECOLE E DEI PRODOTTI PER LA SALUTE

XXIX CICLO

DESIGN AND DEVELOPMENT OF INNOVATIVE CARRIERS FOR DRY POWDER INHALERS

Coordinator: Prof. Marco Mor

Supervisor: Prof. Ruggero Bettini

Tutor: Dr. Francesca Buttini

PhD Candidate: Enrico Salomi

1 Introduction

1.1 Pulmonary drug delivery

Drug administration by inhalation route is a way of delivering drugs that allows achieving directly the therapeutic site for obtaining a local or systemic effect; indeed the inhalation therapy was initially focused on local diseases like asthma and COPD (chronic obstructive pulmonary disease) but now new areas have become of interest for the treatment of infectious diseases like the treatment of cystic fibrosis and tuberculosis (Hickey et al., 2015)(Döring et al., 2012) or for the treatment of systemic disorder like diabetes mellitus with insulin or for delivering vaccines (influenza, measles).

Pulmonary drug delivery presents various advantages; the lung offers a very large area for drug absorption (>100 m^2) plentiful vascularized and characterized by a good epithelial permeability, furthermore the absence of the first-pass effect may increase the drug bioavailability. This aspect along with the fact that the drug is directly deposited on the site of action often results in a significant reduction of the administered drug dose that some time can be even 10 times lower compared to the intravenous or oral dose. For this reason as well as for the significant reduction of the systemic exposure, inhaled corticosteroids and antibiotics have fewer side effects when administered in the lung compared to the oral administration. Moreover, some drugs with a local effect such as

DNAse and hypertonic saline can only reached the target site when administrated by inhalation.

Contrary to other administration routes, the inhalation one requires a pharmaceutical product, which include both the drug formulation and an inhaler device in order to afford the correct deposition of the drug in the lower respiratory tract.

1.2 The respiratory tree

The respiratory tree is a branching system composed by the trachea (generation 0) that bifurcates in a main bronchus for each lung (generation 1) and then continues to bifurcate finishing to the alveolar sacs (generation 23) (Figure 1).

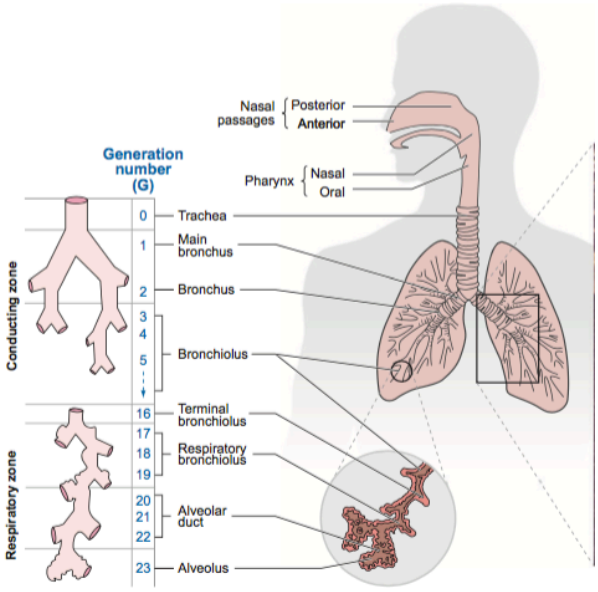

Figure 1 Schematics of the airway generations (Kleinstreuer et al., 2008)

Two main regions can be identified: the conducting airways (generation 0-16) composed by bronchi and non-respiratory bronchioles whose main function is to distribute the air in the peripheral zone and the respiratory airways (generation 17-23) composed by respiratory bronchioles, alveolar ducts and alveoli where gas exchange takes place (Weibel et al., 2005). The conducting airways correspond to less than 5% of the surface area of the lung instead the

respiratory airways comprise the remaining 95%. Clearly the resistance and the air velocity decrease toward the alveoli due to the increase of surface area of the lung.

1.3 Particles deposition in the airways

Particles that travel through the airflow into the lung are subjected to different forces. Many of these particles are deposited in the respiratory tract depending on the size, density, shape, charge, and surface properties of the particles and the breathing pattern of the individual (Groneberg et al., 2003).

Patients inhale medicinal particles for the treatment of respiratory diseases generated from formulations especially designed for this purpose. In contrast to ambient particles, medicinal particles are distributed over a limited size range, their shape and composition are known, and their deposition in the respiratory tract can thus be predicted rather precisely.

Inhaled particles are carried with the tidal air through the respiratory system. However, because of forces acting upon the particles, their trajectories are different from air stream lines. The most important mechanical forces are gravity, inertia, and impulse transfer from collisions with gas molecules. Particles are therefore displaced off stream lines and transported toward the surfaces of the respiratory tract by impaction, sedimentation, interception and diffusion.

Impaction: is the physical phenomenon by which the particles of an aerosol tend to continue on a trajectory when they travel through the airway, instead of conforming to the curves of the respiratory tract (Williams et al., 2011). Particles with high momentum (product of the mass and velocity) are affected by centrifugal force at the points where the airflow suddenly changes direction, and this leads to the collision with the airway wall. This mainly happens in the first 10 bronchial generations, where the air speed is high and the flow is turbulent.

Sedimentation: is the physical phenomenon by which particles with sufficient mass are deposited due to the force of gravity when they remain in the airway for a sufficient time. This predominates in the last 5 bronchial generations, where the air speed is slow and the residence time is therefore longer (Lippmann et al., 1976).

Interception: is the case of fibres, which due to their elongate shape are deposited on the wall of the respiratory bronchioles. Contrary of the inertial impaction, particles subjected to the interception phenomena do not diverge from the stream lines but are deposited as soon as they contact the airways wall (Lippmann et al., 1976).

Diffusion: This is the phenomenon by which the particles of an aerosol move erratically from one place to another in the airways. This happens as a consequence of the Brownian diffusion of particles with size smaller than 0.5 μm when they reach the alveolar spaces, where the air speed is practically zero.

These particles are generally not deposited and they are expelled upon exhalation (Stuart, 1999).

1.4 Parameters influencing particle deposition

The deposition site in the respiratory tract and amount of drug that reaches the respiratory bronchioles are strictly dependant on the particle size, density, shape and hygroscopicity as well as on patient characteristics such as lung function and geometry, age, gender and inspiration flow.

The size of the particles is the main factor that determinates the extent and how the particles will be deposited in the lung; more precisely the particle size distribution is essential to make a prediction in order to evaluate the amount of drug that will be deposited in the airways generation.

Particles shape is not always spherical as most of the solid particles from a dry powder device show an irregular shape. Therefore, the aerodynamic diameter (d_{ae}) is used to make a prediction of the particle behaviour in the aerosol. The aerodynamic diameter of a particle is the diameter of a sphere having unit density and the same settling velocity in the air of the particle of interest. It considers the behaviour of the particle in the airflow, which depends on the size, density and shape of particles.

The aerodynamic diameter value can be calculated by the following equation:

$$D_{ae=}\, D_v \sqrt{\frac{\rho}{\rho_0 \chi}} \quad \text{(Equation 1)}$$

where D_v is the volume of the sphere having an equivalent volume of the irregularly particle; ρ is the particle density; ρ_0 is the unit density; χ is the dynamic shape factor that represents the ratio of actual resistance force on the irregularly shaped particle to the resistance force on an ideal spherical particle having the same volume (De Boer et al., 2002).

For hetero-disperse aerosols, the dimensional distribution is described by the mass median aerodynamic diameter (MMAD), which represents the particle size that divides the mass distribution in half. In addition, in the case of a log-normal distribution, the variability of the particle diameters within the aerosol is represented by the geometric standard deviation (GSD), which is usually calculated by dividing the particle size at the 84^{th} percentile of the cumulative distribution by the median size (Telko & Hickey, 2005).

Hence, it can generally be considered that particles with an MMAD higher than 10 μm are deposited in the oropharynx, those between 5 and 10 μm in the central airways and those from 0.5 to 5 μm in the small airways and alveoli. In contrast particles smaller than 0.5 μm are mostly exhaled by the respiratory airflow (Kirch et al., 2012).

As mentioned before, particles deposition is influenced by several factors such as the shape, density, interpaticulate interaction and hygroscopicity.

The aerodynamic diameter of a particle is a function of the square root of its density. This means that, for a particle with a given geometric diameter, a density reduction will result in a smaller aerodynamic diameter. Thus, it is

possible to use, for example, larger particles that show a good aerodynamic behaviour being at the same time more easily handleable. Shape might be a relevant factor as well. Elongated or needle-shaped particles have aerodynamic diameters that are essentially independent from the length and almost equal to the shortest dimension. Thus, they may exhibit the same aerodynamic diameter of a spherical particle with the same mass or volume.

Furthermore an aspect to consider is that the lung have a relative humidity of approximately 99.5% and the particle size does not remain constant when the particles reaches this region. Particles absorb moisture as they traverse the humid environment of the airways, resulting in increased particle size (Telko & Hickey, 2005).

Moreover, the inhalation product is probably the most complex among the pharmaceutical dosage forms, being composed, not only by the active pharmaceutical ingredient (API) and the formulation, but also by the inhalation device, that is strongly related to the formulation itself.

1.5 Dry powder Inhalers (DPIs)

Dry powder inhalers can be broadly categorized into either passive or active devices (Islam & Gladki, 2008). Passive DPIs are breath-actuated, deriving the energy for powder dispersion and aerosol formation solely from the patient's inspiratory manoeuver. However, patients can produce a wide range of flow rates, which is reflected in the high inter-patient variability in the dose delivered

from these devices. Additionally, some patients can only generate flow rates too low to produce an aerosol cloud, and treatment with DPIs can be ineffectual. In light of this, many DPI developers have concluded that the best strategy lies in decoupling powder dispersion from inhalation and incorporating an assortment of auxiliary energy that allow dispersion upon inhalation at a reasonable flow rate and have flow rate independence; an example of this is reported by Buttini et al. (2016) that demonstrated a consistent drug detachment independent of the applied flow rate from the NEXThaler® device (Figure 2); the results should be attributed to the presence of release mechanisms activated by the inspiration of the patient namely the Breath Activated Mechanism (BAM). The presence of BAM implies that the powder is released only when a specific threshold of inspiration flow rate value is attained (35L/min), this effect results in an instantaneous release of the drug (0.35 s) that makes irrelevant the following part of the patient inspiration flow rate.

Figure 2 Multi-dose NEXThaler by Chiesi Farmaceutici

DPIs can be further classified as either single dose or multi-dose devices, the latter being delineated into multi-unit dose or reservoir inhalers (Colombo et al., 2013). The single-dose inhalers represent the first generation of DPIs (Spinhaler™, Rotahaler™), although some devices in this category are still currently marketed (Aerolizer™, Handihaler™). These inhalers generally deliver

the dose from a hard capsule inserted into the device prior to each actuation. The multi-unit dose inhalers disperse individual doses pre-metered by the device manufacturer into blisters, while reservoir DPIs contain enough powder for multiple doses (typically 60 - 200) within the device, metering individual doses prior to actuation. Advantages of DPIs employing factory-metered doses include environmental protection of the powder and consistency of the dose relative to their reservoir counterparts. Regardless of how the dose is provided, all DPIs contain a de-agglomeration principle to address the challenges to produce aerosols from a dry powder.

The only request that every device must satisfy is specified by the United States (USP37-NF 30, Chapter 601) and European (Ph. Eur. 8.0, 2.9.18.) Pharmacopoeia that instruct to draw 4L of air through the DPI under evaluation at a flow rate that produce a pressure drop of 4 kPa across the device. Thus, as illustrate in the equation 2, the device intrinsic resistance R is equal to the square root of pressure divided by flow rate.

$$R = \frac{\sqrt{kPa}}{(L/\min)} \quad \text{(Equation 2)}$$

Therefore, a device with a high intrinsic resistance requires a low flow rate to generate a pressure drop of 4 KPa across the device instead a device with a low intrinsic resistance requires a high flow rate to generate the pressure drop illustrated in the pharmacopoeia. The principle behind the device resistance is

the Venturi law, for which a fluid flux increases its velocity through a constricted section, that, for the device, is represented by the air inlet (Figure 3).

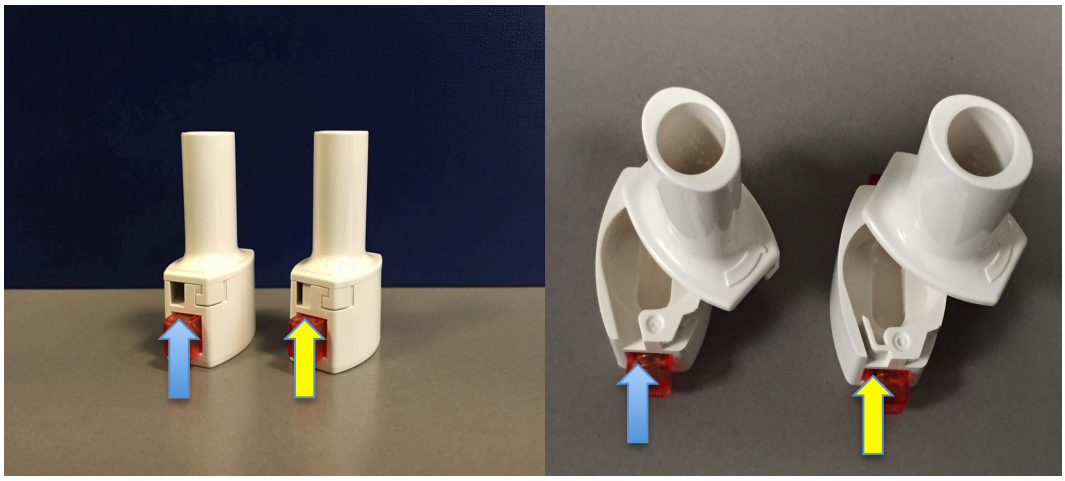

Figure 3 Picture of Plastiape RS01 device (ITA). On the left-hand side a low resistance device with a wide air inlet, on the right-hand side a high resistance device with a tight air inlet

The aerosolization performance of a formulation-device combination is commonly evaluated through in vitro deposition tests by using the impactors recommended by the Pharmacopoeia (Ph. Eur. 8.0, 2.9.18.). The aerodynamic assessment methods allow determining the fine particle dose (FPD), namely the amount of drug particles with an aerodynamic (or cut-off) diameter lower than 5 µm. From the ratio of the FPD to the emitted dose (ED, the quantity of drug exiting the device after inhalation), it is possible to obtain the fine particle fraction (FPF) that is commonly used to evaluate DPI performance.

1.6 Traditional DPI formulations

To be effectively delivered into the lung, drug particles are generally required to fall in the size range between 1 - 5 µm (Pilcer et al., 2012); particle size reduction is typically performed through "top down" processes such as jet milling, which yields highly cohesive particles with ill-defined size distributions

and morphologies (Crowder et al., 2001). Particle engineering, a “bottom up” approach to produce respirable size particles at the initial particle formation step, holds promise in addressing the drawbacks of attrition processes such as jet milling. However, few technologies have been industrialized at least in part due to the increased cost of goods for these nascent techniques (Chow et al., 2007). The cohesive interactions between the powder particles arise from a combination of electrostatic, capillary, and van der Waals forces, although by allowing the particles enough time to dissipate excess electric charges, and in the absence of high relative humidity, the latter are most important. Individually weak, but collectively robust, van der Waals interactions are the dominant attractive forces in particles with diameters below 10 μm, exerting a “velcro effect” that impedes powder dispersion. To aid in the entrainment and de-agglomeration of these cohesive particles, dry powder formulations are generally binary, or adhesive, blends, with the bulk, > 95% (w/w), comprised of large inert carrier particles (50 - 100 μm), to improve the flowability and metering properties of the formulation (De Boer et al., 2003). However, while the addition of the large carrier particles allows the powder to be readily entrained in a flow stream, the adhesive interactions between the drug and carrier hinders the formation of an aerosol comprised of primary drug particles. Consequently, drug particles that fail to detach from the carriers are deposited in the throat and upper airways.

1.7 Particle engineering technologies

In lieu of developing inhalers that can enhance the de-agglomeration forces, an alternative approach is to reduce the cohesive and adhesive interactions within the powder through modifications to both drug and carrier particles (Frijlink & de Boer, 2005). For micronized drug, one strategy is to increase the diameter of the particle, thereby lowering the surface area-to-volume ratio, without compromising its aerodynamic diameter. From the above, it can be seen that an increase in the diameter of a particle can be balanced by a concomitant reduction in its density, an approach embodied by the large porous particles (Edwards et al., 1997).

Additional developments in powder dispersion performance include smaller porous particles, Pulmospheres (Figure 4), and the use of supercritical fluid technology. However, in comparison to unmodified drug, these particles can be costly to manufacture, requiring the use of spray drying or spray-freeze drying (Frijlink & de Boer, 2005). Moreover, given their increased volume, larger reservoir systems must be developed to accommodate the formulation, requiring the production of devices specific to the powder (Frijlink & de Boer, 2005).

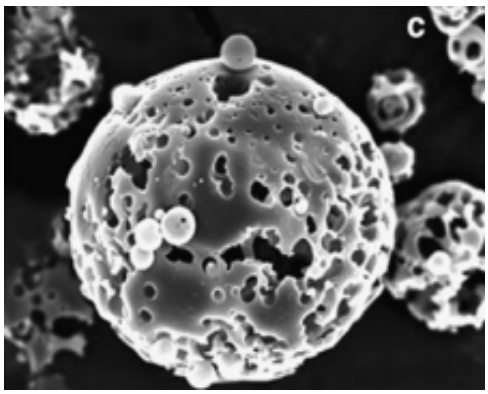

Figure 4 Porous tobramycin particles, Pulmosphere™ (Geller et al., 2011)

Another strategy to overcome the issues related to the reduced dimension of drug particles is the controlled agglomeration into soft pellets by spheronization (Claus et al., 2014)(Figure 5). These loose agglomerates are composed by primary microparticles held together by weak interactions. Soft pellets are strong enough to be handled but, thanks to the turbulence generated during inhalation, they can easily break up into primary particles of respirable size (chimerical agglomerates).

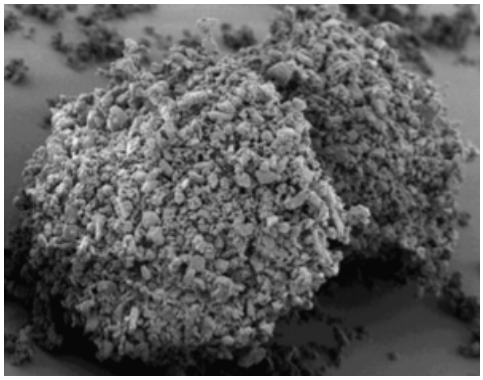

Figure 5 Soft pellets from pulmicort® turbohaler® (Hoppentocht et al., 2014)

Thus, while particle engineering technologies have demonstrated the ability to markedly improve aerosol performance from traditional dry powder inhalers, at present, marketed DPI formulations are generally binary formulations (adhesive mixture) that exhibit poor dispersion properties relative to the aforementioned particle technologies. Accordingly, to improve performance of a DPI therapeutic regimen, strategies to optimize both the formulation and device are required. What follows is a detailed discussion of the physicochemical properties of binary DPI formulations, particularly the parameters of the carrier particle population that have been examined in the literature and found to either enhance, or impair performance through various mechanisms.

1.8 Parameters governing performance of binary blends

As mentioned above, therapeutic formulations administered via dry powder inhalers are typically interactive mixtures, comprised of the active pharmaceutical ingredient and a coarse carrier material blended together to produce a homogeneous powder. Delivery to the deep lung requires drug particles possessing aerodynamic diameters between 1 and 5 μm. However, given the high surface area-to-volume ratio of particles in this size range, van der Waals forces dominate the interactions, producing highly cohesive powders that flow poorly and are consequently resistant to re-dispersing back into primary particle sizes during inhalation. Drug agglomerates that fail to de-aggregate sufficiently deposit in the mouth and throat, reducing the therapeutic efficacy of the treatment and increasing the potential of unwanted side effects. To improve powder flow and dispersion, as well as assist in dose metering, a population of coarse particles (50 – 100 μm) are incorporated into the formulation, typically in excess of 95% (w/w) to serve as carriers onto which the drug particles adhere during blending, and from which they are subsequently detached during inhalation (Dickhoff et al., 2005). Carrier particles must be inert, possess a physical and chemical stability compatible with the drug substance, and be readily available and inexpensive (X. Zeng et al., 2001). While a variety of materials, primarily sugars, have been evaluated in the literature for their suitability to serve as carrier particles, α-lactose monohydrate is the only material currently approved for inhalation purposes

(Hooton et al., 2006)(Steckel & Bolzen, 2004). Production of a stable and homogeneous powder blend requires that the interaction between drug and carrier particles would be balanced, with forces strong enough such that drug preferentially adheres to the carrier during mixing, yet sufficiently tenuous to facilitate re-dispersion of drug particles during inhalation (Begat, et al. 2004). Formulation factors affecting overall performance include the drug substance and concentration, mixing rate, mixing time, batch size, and the carrier particle population (Saleem et al., 2008).

Then, the delivery of the drug takes place through three different processes: the detachment from the carrier (which remains in the inhalation device or deposits in the oropharyngeal region), the dispersion in the airflow and the deposition in the respiratory tract (Figure 6).

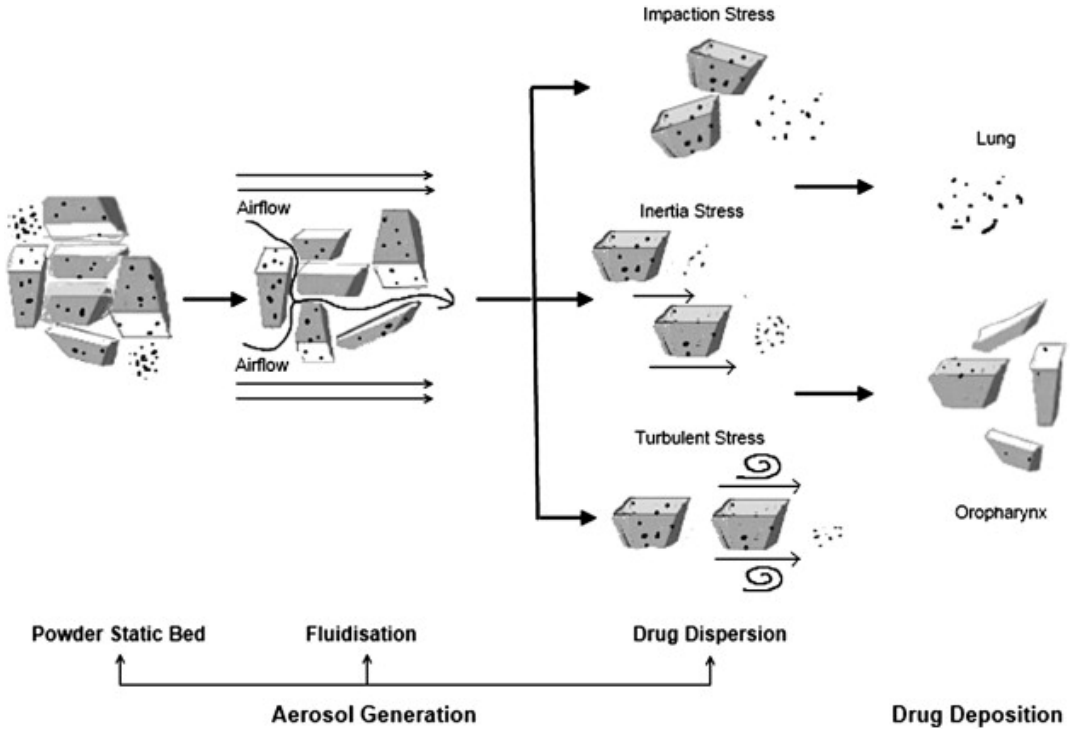

Figure 6 Aerosol generation and drug deposition (Pilcer et al., 2012)

1.8.1 Interpaticulate interaction

When considering adhesive mixtures, the study of the interactions between carrier and drug is of paramount importance for a good understanding of the processes that finally determine the performance of the product. One of the most problematic aspects is represented by the presence of inter-particulate forces that prevent the disaggregation of the powder, thus compromising the efficiency of drug delivery into the lungs. These inter-particulate interactions (both cohesion between drug-drug particles and adhesion between carrier-drug particles) are the result of physical and chemical forces: van der Waals (proximity) forces and mechanical interlocking due to the presence of defects (e.g., clefts and asperities) on the surface of the carrier, electrostatic and capillary forces, forces deriving from the presence of impurities or amorphous regions, specific (acid-base) interaction forces and hydrogen bonding (Hickey et al., 2007) (Figure 7).

In carrier-based formulations, the size difference between a micronized drug particle and a carrier particle allows to consider their interaction (adhesion) as that between a sphere and a flat surface. Van der Waals and electrical forces are proportional to the diameter of the micronized drug particle and vary with its distance from the carrier. Capillary forces are affected by the surface tension of the liquid between particles (Pilcer et al., 2012).

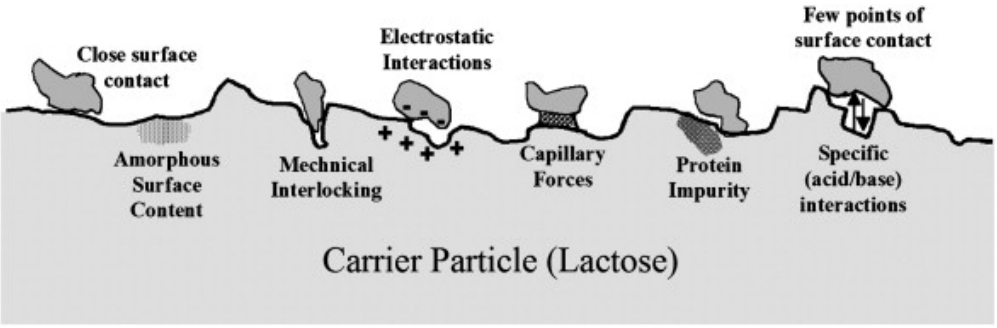

Figure 7 Illustration of the different causes of interaction between micronized particles (drug) and lactose carrier particles (Pilcer et al., 2012)

Van der Waals forces are low attractive dipole-dipole forces and are the most dominant inter-particulate interactions determining adhesion and cohesion within a powder formulation. Being dependent on the distance between particles, these forces are influenced by surface roughness. Highly corrugated surfaces with pronounced asperities may increase the distance between two particles and limit van der Waals interactions. On the other hand, van der Waals forces strongly increase in the case of large contact areas when, for example, protuberances fit into cavities (mechanical interlocking).

Capillary forces are attractive forces related to the formation of a concave-shaped meniscus (liquid bridge) due to the condensation of water vapour around the contact area of two contiguous surfaces. The intensity of such forces is affected by surface characteristics (e.g., roughness and physico-chemical properties) and, overall, by the environmental relative humidity.

Electrostatic interactions can be attractive or repulsive depending on whether they involve particle with opposite charge or the same charge respectively. Electrostatic charges arise from triboelectrification that is a type of contact electrification in which certain materials become electrically charged after being

brought into contact by short collision or by intense friction. Triboelectrification mainly occurs as a consequence of manufacturing processes such as mixing and handling, but can appear also during the fluidization of the powder bed inside the inhaler device. Electrostatic interactions are relevant in the formation and maintenance of the adhesive mixture, the detachment of drug particles from the carrier and their deposition in the respiratory tract (electrostatic interception). Moreover, they can be strongly influenced by relative humidity. During storage, high RH conditions may lead to a reduction of electrostatic interactions, since the formation of water layers around particles enhances the surface conductivity and favours the dissipation of the charges. On the other hand, these conditions favour capillary condensation and, consequently, stronger capillary interactions. The above-described physical interactions are barriers to the aerosol generation. In an ideal formulation, the adhesive interaction between carrier and drug particles should be overcome by the external forces (e.g., inertial, lift, drag, friction and shear forces) produced by the inspiration airflow through the inhaler. Unfortunately, due to the complexity and heterogeneity of powder systems, it is extremely difficult to consider and control each type of interaction separately.

1.8.2 Surface roughness

Carrier particles with larger diameters possess a great surface roughness, thus affording drug particles shelter from detachment mechanisms relying on

acceleration flow or impaction of drug aggregates on a surface (De Boer et al., 2003). Drug particles will accumulate in the discontinuities on the carrier particle surface, and a rougher surface potentially affords multiple contact points between the drug and carrier, increasing the adhesive force between the particles (Podczeck, 1998). This view is supported by studies investigating the influence of carrier morphology, where smoother lactose carriers produced higher fractions of fine particle deposition (X. Zeng et al., 2001)(Ferrari et al., 2004; Young et al., 2002). An additional role of surface roughness was proposed by Podczeck, who believed that detachment of fine drug particles from the surface of coarse carriers occurs laterally to the surface, where the drug will slide until it reaches the edge of the carrier and fall-off (Podczeck, 1998). The adverse influence of carrier particle size is then obvious, as it will extend the distance the drug particle must travel prior to detachment, requiring greater aerodynamic drag forces relative to a smaller carrier particle. However, this theory is contested by reports indicating that elongated lactose carrier particles can improve dispersion performance (Kawashima et al., 1998). The authors attributed this beneficial influence to the enhanced aerodynamic properties of the elongated particles, allowing them to travel longer distances than their equivalent volume-spherical counterparts and prolong the exposure of adhered drug particles to drag forces.

When examining the detachment mechanisms, it is evident that smoother particles allow for greater detachment by flow and aggregate impaction,

whereas detachment by mechanical forces is largely independent of carrier particle surface rugosity. Accordingly, for rough surfaces detachment becomes less dependent on flow and aggregate impaction, relying more on mechanical forces. Thus, it is not that high surface rugosity would inhibit detachment entirely, but rather it shifts the detachment mechanism to mechanical forces. As such, it could then be theorized that the size ranges examined (63 – 90 μm) in the study investigating surface roughness might be too small to permit a significant contribution of detachment to arise from carrier particle collisions (Podczeck, 1998), (Kawashima et al., 1998). Impaction forces require both sufficiently high flow rates coupled with a relatively large carrier particle diameter. As an example, two spherical carrier particles, one 90 μm and the other 350 μm (X. Zeng et al., 2001)(Dickhoff et al., 2005), moving with comparable velocity, impacting directly with a surface can be considered. In this case, the momentum difference between the two particles is entirely dependent on their mass, which is related to the diameter, thus increasing the carrier particle size from 90 to 350 μm, could potentially produce impaction forces greater in the latter carrier particle; assuming similar particle velocities. In summary, carrier particle roughness may inhibit performance by causing a shift to a detachment mechanism highly dependent on mechanical forces. Small carrier particles may possess insufficient mass for these forces to be effective at a given flow rate. In contrast, surface roughness of very large carriers is less debilitating when compared to that of smaller carriers, as the mechanical forces

generated may potentially dominate over the detachment mechanisms that require a smooth carrier surface for optimal performance.

1.9 Ternary mixture

Addition of fine excipient material to a carrier based dry powder inhalation mixtures has proved to have a positive effect on the aerodynamic performance of the drug.

Formulations containing an increased percentage of fines improved the drug detachment (up to a certain threshold value); in fact, with further increase in fine concentration the FPF remains constant or decreases. As a general rule, therefore, in addition to the drug and the coarse carrier, fine material is often present in DPI mixtures, either as an extrinsic added fraction of fines or as intrinsic fines within the coarse carrier. However, the exact mechanism for how these fine lactose particles alter the formulation performance has remained unclear with different theories attempting to explain the phenomenon.

Figure 8 illustrates the two main theories that explain how the fine excipient material improves the drug detachment.

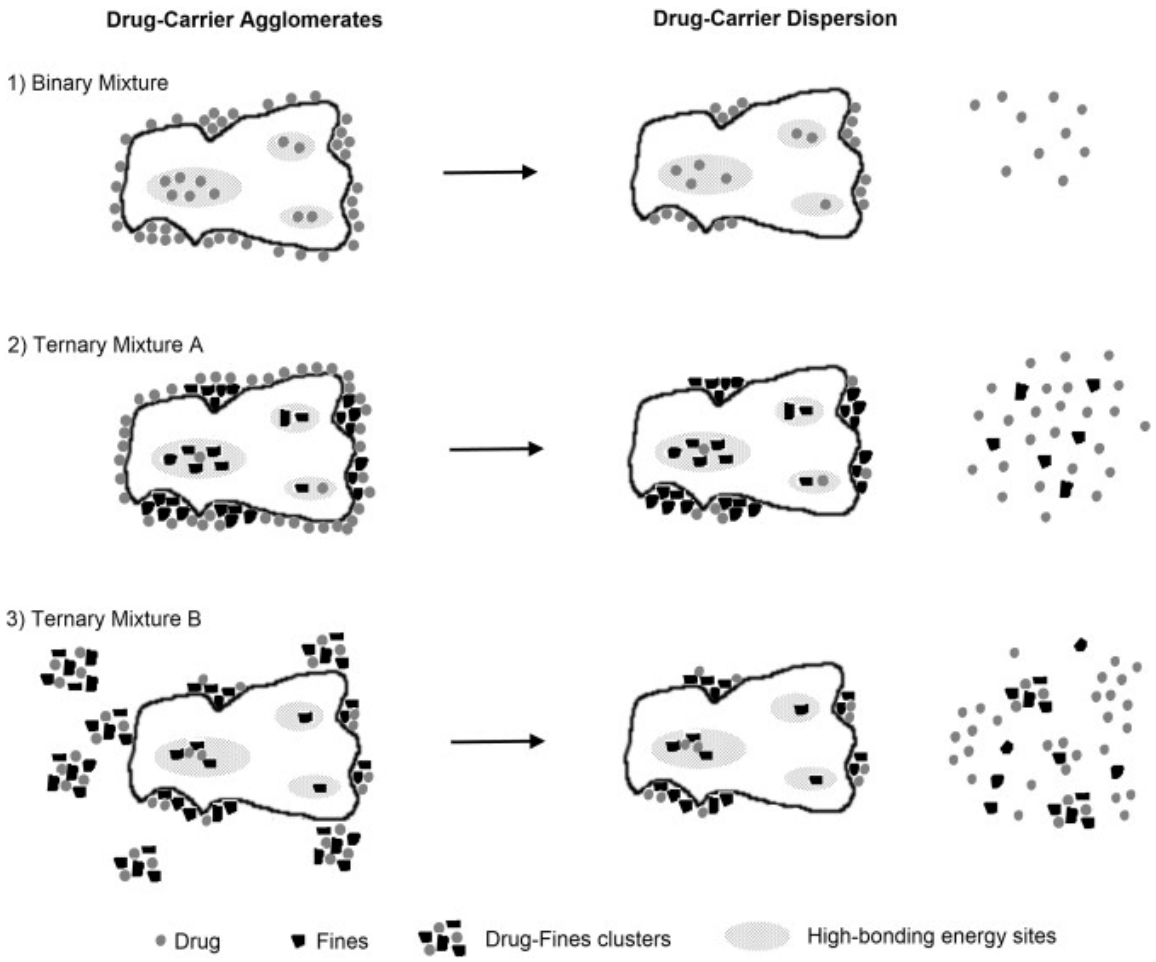

Figure 8 Mechanisms of drug dispersion from 1) binary mixture, 2) ternary mixture, active site theory and 3) ternary mixture, agglomerate theory (Pilcer et al., 2012)

The *active site* theory postulate that fine excipient material bind the high energy sites on the course material leaving the low energy site for drug-carrier adhesion; there are several studies that tested this hypothesis, X. M. Zeng et al., (1999) reported that a mixture prepared blending course particle and fine material prior to the addition of the drug resulted in better drug detachment compared to a formulation prepared by blending coarse particles with drug prior to fine material addition; In contrast to this work Louey & Stewart (2002) and Lucas et al. (1998) reported that the addition of fine material is independent of the blending order and thus resulting irrelevant for drug detachment.

The *agglomerate* theory suggests that the drug particles form agglomerates with fine excipient material redistribute on the carrier surface making more easily the drug aerosolization and deposition. More recently, it has been shown that the relationship between blending order and fine particle delivery might be influenced by drug concentration and mixing time (Jones et al., 2010); this led the authors to suggest the "agglomerates" theory as more appropriate to explain the observed behaviour.

Finally, in recent year other theories have been proposed about the role of fine material. The *fluidization enforcement* theory explains the fine excipient effect on powder bed fluidization; a decrease of air permeability in coarse particles results from filling the coarse particles holes by the fine excipient material that leads to higher aerodynamic behaviour of carrier and consequently to a higher drug detachment (Le et al., 2010; Watling, et al., 2010).

Another mechanisms are also speculated. Fine materials below a certain size may lower dispersion performance by increasing the effectiveness of press-on forces arising during the mixing process and/or through the formation of coherent fine particle networks containing the drug particles on the carrier surface (Grasmeijer et al., 2014).

1.10 Lactose and solid state

Lactose is a disaccharide composed by β-D-galactose and α-β-D-glucose fragments linked by a β-1-4 glycosidic bond (Jawad et al., 2012).

Lactose may exist in different forms, which differ one from the other from the configuration of the anomeric Carbon (C1) that generically are defined polymorph (Figure 9). The polymorph for definition is a material that exhibits different crystal structures within the solid state but has identical characteristics in solution.

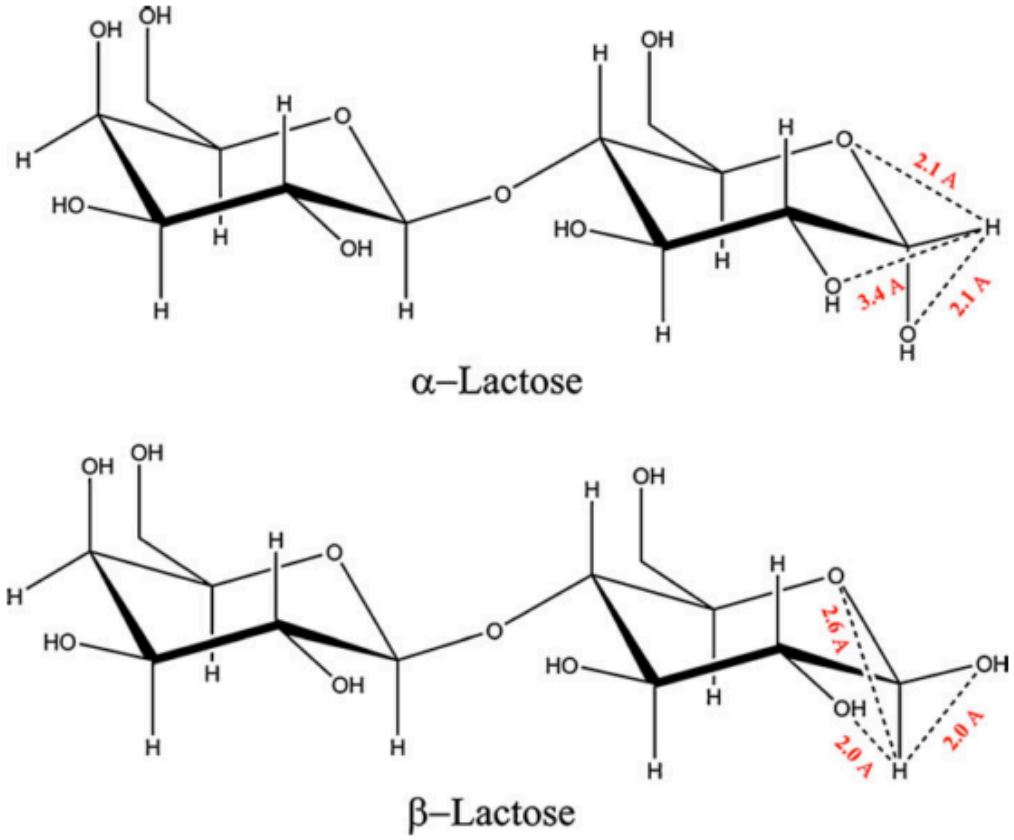

Figure 9 Representation of two anomers of lactose (Jawad et al., 2012)

This definition is no strictly applicable for lactose. Is true that lactose exists in different crystal structures in solid form but an interconversion between the α and β forms occurs in aqueous solution, where mutarotation takes place until equilibrium is reached (α/β 37:63 at neutral pH and room temperature). Nevertheless, since the different forms of lactose are widely described as polymorph the terminology will be maintained (Kirk, et al., 2007).

Therefore, there are four well-accepted lactose forms. These consist of a single hydrated form, α-lactose monohydrate (L$\alpha \cdot H_2O$) (Haque, 2005; Jones et al., 2012) and three dehydrated forms, β-lactose (Lβ) (Lehto et al., 2006), stable anhydrous α-lactose ($L\alpha_S$) (Chen et al., 2015) and unstable hygroscopic anhydrous α-lactose ($L\alpha_H$) (Listiohadi & Hourigan, 2009); alternatively lactose can be amorphous with variable anomeric composition.

α-lactose monohydrate is the most commonly use as a coarse or fine excipient material in DPIs formulations due to its stability and relatively non-hygroscopic characteristics. Therefore, the chemical characterization of lactose is an important variable that should always be investigated since differences in the physical properties of the different forms could be considered a significant source of potential variation that might be responsible for batch-to-batch irreproducibility

2 Aim of the project

The aim of the present thesis work was to investigate and set-up novel method to produce, lactose granules suitable to be used as carrier in adhesive mixture with micronized active ingredients for pulmonary administration.

In particular, the goal was the set-up of a new method capable to produce lactose with controlled physico-chemical characteristics affording efficient and reproducible aerosolization performance when used as a carried in binary blends with micronized active ingredients.

As a matter of facts, the two main producers, namely DFE Pharma and Meggle, supply lactose for inhalation not customized and not engineered; this sometime imply some disadvantages such as possible small differences among production batches of the same raw material which are not detected by the standard test for assessing compliance with the Pharmacopoeia requirement. However, these differences may affect the aerodynamic behaviour of micronized active ingredients aerosolized from adhesive mixture made with these lactose batches. Therefore, many companies involved in pulmonary drug delivery are interested in the production of customized and engineered lactose particles with more reproducible properties at the microscale and with optimized characteristics for aerosolization.

The strategy adopted to achieve the goal was focused on the production of customized porous lactose granules, having a controlled surface area as well as

reproducible and suitable flow properties. The first characteristic influences the capability to form adhesive mixture with adequate doses of active ingredient, while the second one, affects the aerosolization performance and the powder workability.

The strategy was pursued by designing and developing an innovative microwave drying process which introduced also the advantages of process rapidity and scalability.

Lactose granules were fully characterized for fort their physical properties by using proton nuclear magnetic resonance (^{1}H NMR), X-ray powder diffraction (XRPD) and differential scanning calorimetry (DSC) and compared with the starting material, furthermore different formulation approaches using two model drugs were examined, one hydrophilic, the β2 adrenergic receptor agonist salbutamol sulphate and on lipophilic the anti-inflammatory glucocorticoid beclomethasone dipropionate.

3 Materials and methods

3.1 Materials

3.1.1 Lactose

Three lactose powders were used as starting materials: Lactohale LH100 and Respitose ML006 by DFE Pharma were provided (Germany) while Inhalac 50 was provided by MEGGLE (Germany). Table 1 reports the particle size distribution of these materials according to the producer.

Table 1 particle size distribution of lactose raw materials according to the producers.

	dv10 (µm)	dv50 (µm)	dv90 (µm)
Lactohale LH100	45-65	125-145	200-245
Respitose ML006	2	17	45
Inhalac 50	130-180	230-290	320-370

Coarse lactose Capsulac (dv50 = 212-355, batch #B0043) provided by Chiesi Farmaceutici (Italy).

Two types of Lactose fine, Lactohale LH300 (dv50 ≤ 5 µm, dv90 ≤ 10 µm) provided by DFE Pharma and Preblend Chiesi (constituted by 98% w/w of Inhalac 120, Meggle, and 2% w/w of magnesium stearate (MgSt) batch #1008513) provided by Chiesi Farmaceutici (Italy) were employed during the project development.

Moreover, three types of Lactose "fine" starting from Lactohale LH100 were selected by sieving in order to obtain three different size of fine lactose. In this case, the word "fine" is it intended with the purpose of differentiate this kind of lactose from the granular lactose. The size of "fine" lactose obtained is listed below:

- "fine" lactose < 45 μm;
- "fine" lactose < 65 μm;
- "fine" lactose < 125 μm.

3.1.2 Fine Excipient

Magnesium stearate (batch #123728) was provided by Chiesi Farmaceutici.

MgSt is a salt composed by two equivalent of stearate (anion) and the cation magnesium. It is used form many purpose in the pharmaceutical industry as lubricant, anti-adherent or for dry coating process.

3.1.3 Active Pharmaceutical Ingredient (API)

3.1.3.1 Salbutamol Sulphate (SS)

Salbutamol sulphate (dv50 = 2.7 μm) was supplied by Teva Pharmaceutical Industries (Israel). Salbutamol sulphate (Figure 10) is a selective β_2 adrenergic receptor agonist used as a bronchodilator in the treatment of asthma and COPD and was chosen as model drug with hydrophilic characteristics (LogP = 0.34, Drugbank.ca).

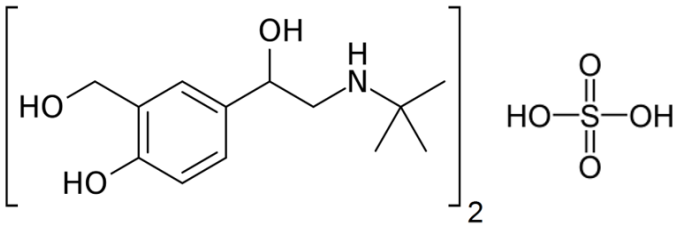

Figure 10 Molecular structure of Salbutamol Sulphate

3.1.3.2 Beclomethasone Dipropionate (BDP)

Beclomethasone dipropionate (dv50 ≤ 2 μm) by Chiesi Farmaceutici (Italy) was provided.

BDP (Figure 11) is an anti-inflammatory glucocorticoid used for the treatment of asthma and COPD was selected as model drug with lipophilic characteristics (LogP = 1.3, Pubchem.ncbi).

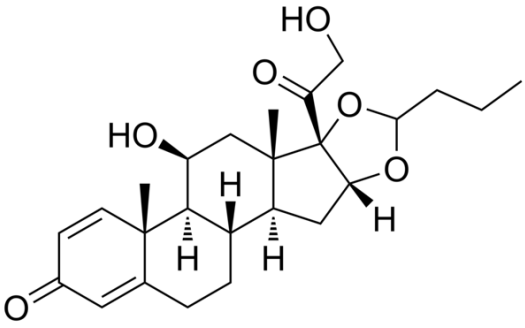

Figure 11 Molecular structure of Beclomethasone Diipropionate

3.2 Methods

3.2.1 Investigation of novel methods to produce a lactose carrier for inhalation

3.2.1.1 Procedure #1: Microwave preparation of lactose granules using water as binder solution

Lactohale LH100 was wetted with a different amount of water in order to obtain a slurry.

Slurry samples were prepared by mixing the following amount of lactose and water with a mortar:

- 2g di LH100 + 5% w/w H_2O;
- 2g di LH100 + 10% w/w H_2O;
- 2g di LH100 + 15% w/w H_2O;
- 2g di LH100 + 20% w/w H_2O.

All the slurries were put in a 50 ml capacity crystallizer and then dried in the microwave (MicroFAST-Microwave-Vacuum Moisture Analyzer, Milestone, USA) at 250 Watt for 5 minutes.

A further investigation with a design of experiments (DoE) method was evaluated to speed-up the research plan in order to identify significant factors affecting the process and the product quality attributes. The optimisation was based on three process factors, namely water percentage, microwave power (W) and drying time (min). Given that three input variables at two levels were

considered for the selected material, a fractional factorial 2-level DoE was adopted using THE UNSCREMBLER® X 10.3 software (Camo software, Norway) for the study. The 2-level design incorporating 3 parameters plus two central points required $2^3 + 2 = 10$ total experiments for each material to be tested. To investigate how the process affects the material performance, this experimental research was focused on the three outputs: 1) percentage of water lost during the microwave drying process; 2) yield of the process (% of powder with size >180 µm, as determined by sieving and 3) friability determined using a modified friability test for tablets (Ph. Eur. 8.0 2.9.7). Here the friability test was carried out by substituting the standard cylinder of the friabilometer with a plastic jar having a volume of 100 ml rotated at 100 rpm for 4 minutes after loading in the apparatus the total amount of powder resulting from the sieving through the 180 µm sieve.

3.2.1.2 Procedure #2: Microwave preparation of lactose granules using an almost saturated lactose solution as binder

Lactose preparation was carried out by mixing the lactose powder with 15 % (w/w) of an almost saturated lactose solution as a binder instead of water as described in the *procedure #1* (chapter 3.2.1.1). The almost saturated lactose solution was prepared by dissolving under stirring at 50 ° C, 3.5 g of lactose in 10 mL of ultrapure water (resistivity = 1-10 MΩcm, conductivity = 1-0.1 µS/cm). Thereafter the slurry was prepared and was granulated by forcing the wet mass

through either a 212 μm or a 425 μm sieve. The obtained granules were then dried in the microwave at 600 W for 5 minutes.

This procedure was carried out with a slight variation consisting in the selection of a Lactohale having particle size higher than 125μm as staring material for the granules production.

3.2.1.3 Procedure #3: Vacuum oven preparation of lactose granules using an almost saturated lactose solution as binder

The lactose raw material was wetted with a 15% w/w the almost saturated lactose solution. The slurry was granulated passing through either a 425 μm or a 600 μm sieve and then the granules were dried in an oven (Gallenkamp, Fistreem International LTD, UK) for 30 minutes at 60°C with vacuum of 200 mbar residual pressure. The samples were then weighted in order to evaluate the weight loss, hence, the drying was repeated for 5 minutes in order to assess that no further weight loss occurred.

3.2.1.4 Procedure #4: Microwave preparation of Lactose granules + "fine"[1] lactose using an almost saturated lactose solution as binder

The addition of a "fine" portion of lactose to the carrier was investigated in order to improve the respirability of the drug. The "fine" portion was added using different method:

[1] The word "fine" has to be considered here as non-granular lactose

Method #1

Three different "fine" materials produced starting from Lactohale LH100 were investigated:

- "fine" lactose <45 μm;
- "fine" lactose <65 μm;
- "fine" lactose <125 μm.

The procedure was carried out manually and the "fine" portion was blended with LH100 raw material before the carrier preparation. In detail, lactose LH100 was mixed manually in a mortar with 5, 10, 30 or 50% w/w of the selected "fine" material. Then, the slurry was prepared with a 15% w/w of almost saturated solution of lactose LH100 (35% w/v lactose in water), thus the slurry was granulated through a size of 425 μm and dried in the microwave at 600 W for 5 minutes.

Method #2

The portion of fine lactose either LH 100 < 45 μm produced starting from LH100 (selected by sieving as reported above), LH 300 or Preblend Chiesi was added at 10% w/w directly to the dried LH100 granules (425 μm size) after the slurry preparation carried out as describe in *procedure #2*.

3.2.2 Proton Nuclear Magnetic Resonance (^{1}H NMR)

^{1}H NMR spectra were recorded in DMSO-d_6 at 25 °C using a Bruker AV400 spectrometer (Bruker, USA). The anomeric composition of each sample of lactose was determined by integrating the peaks at δ = 6.3 ppm and δ = 6.7 ppm,

corresponding to the protons of the hydroxyl group at carbon C1 in the α- and β-anomer, respectively (Jawad et al., 2012). Spectra were processed using MestReNova software (Mestrelab Research, Spain). An apodization of 0.2 Hz was applied and spectra were manually phase corrected prior to automatic baseline correction and final peak integration. The anomeric composition of the tested lactose was calculated as the ratio between the two peaks corresponding to the α- and β-anomer.

3.2.3 X-Ray Powder Diffraction (XRPD)

The patterns of X-ray diffraction on powders were recorded on a MiniFlex diffractometer (Rigaku, Japan) using Cu K_α radiation (λ= 1.5418 Å) generated with 30 kV. The samples of lactose powder were transferred into the sample holder until it was completely full and then pressed with a glass slide in order to obtain a flat and homogeneous surface. The goniometer was set at a scanning rate of 1.5 ° min^{-1} (step size = 0.05 °) over the 2θ range 2-40 °.

3.2.4 Differential Scanning Calorimetry (DSC)

DSC measurements were performed using an Indium calibrated (onset of melting T_m = 156.48 °C, enthalpy of melting ΔH_m = -28.60 J g^{-1}) DSC 821e instrument (Mettler Toledo, Switzerland) driven by STARe software (Mettler Toledo). DSC traces were recorded by placing accurately weighed quantities (6-12 mg) of powder samples in a 40 µL Aluminium pan which was then sealed and

pierced twice. Scans were performed between 25 and 250 °C at a scanning rate of 10 °C min^{-1} under a purging nitrogen atmosphere (100 mL min^{-1}).

3.2.5 Scanning Electron Microscopy (SEM)

Lactose carrier morphology by scanning electron microscopy was assessed by using a SEM SUPRA 40 (Carl Zeiss, Germany). Each powder sample was placed on a conductive sample holder previously covered with a double-sided conductive carbon tape so as to allow the dispersion of the charge. Particles in excess were removed by a gentle flow of nitrogen.

The samples were analysed in high vacuum conditions and the images were collected at different magnifications using a voltage of 1.5 kV.

3.2.6 Preparation of beclomethasone dipropionate/lactose binary blends: Sandwich method

BDP and the various lactose powders were mixed in a ratio 1:100 (w/w) to obtain 5 g of binary mixture. The formulation was blended at a constant speed of 32 rpm for 30 min with a Turbula® T2A shaker-mixer (WAB, Switzerland) using a grounded stainless steel vessel (internal volume = 40 mL, internal diameter = 5 cm, height = 4,5).

After 30 minutes the blend was sieved using a sieve mesh slightly greater then carrier particle size to remove the drug agglomerates and re–blended at 32 rpm for 15 min.

3.2.7 Preparation of salbutamol sulphate/lactose binary blends

Salbutamol sulphate (SS) and lactose were mixed in a ratio 1:10 (w/w) in order to obtain 5 g of binary mixture; the formulation was blended at a constant speed of 32 rpm for 30 min with a Turbula® T2A shaker-mixer (WAB, Switzerland) using a grounded stainless steel vessel (internal volume = 40 mL, internal diameter = 5 cm, height = 4,5).

After 30 minutes lactose was added to obtain a mixture in a ratio 1:40 and re – blended at 32 rpm for 30 minutes. Thereafter, the remaining lactose was added to obtain a binary mixture in a ratio 1:100 (w/w) and re - blended at f 32 rpm for 60 minutes.

3.2.8 Ternary mixtures

Five grams of each formulation were prepared by mixing coarse and fine lactose in Turbula® at 32 rpm for four hours, then the carrier was mixed with the API as described in section 3.2.6 and 2.2.7

3.2.9 High drug doses blends

Both binary and ternary BDP blends (size batch 5 g) containing 10% drug were prepared according to a 4 steps procedure:

- sieving 0.5 g of BDP with half part of the carrier; BDP/carrier was gently forced through a 600 μm sieve . Thereafter the remain part of the carrier was added;

- mixing in Turbula® mixer for 30 min at 32 rpm;
- sieving again through 600 μm;
- mixing with Turbula® for other 15 min.

In the case of ternary mixture the carrier was constituted by a blend of course and fine lactose prepared by pre-mixing them in Turbula® for 2 hours at 32 rmp.

3.2.10 UV Analysis of Salbutamol Sulphate

The quantitative analysis of salbutamol sulphate was performed by UV spectroscopy. Measurements were carried out with a V-530 UV-Vis/NIR spectrophotometer (Jasco, Japan). The absorbance of each sample was determined at λ = 224 nm using quartz cuvettes with optical path of 1 cm. For each sample three quantitative determinations were carried out, each of which was obtained as the average of ten consecutive readings. The analytical method was validated for linearity of the response (absorbance *vs*. concentration) in the concentration range 1.45-43.00 μg/mL using water as solvent, limit of detection (LOD = 0.37 μg/mL) and limit of quantification (LOQ = 1.11 μg/mL). A calibration curve (absorbance *vs*. concentration) was also built to evaluate the UV response of the capsules employed in the *in vitro* aerodynamic assessment. The linearity of the response was assessed in the concentration range 1.85-6.60 mg/mL (LOD = 0.27 mg/mL, LOQ = 1.32 mg/mL) using water as solvent.

3.2.11 HPLC Analysis of beclomethasone dipropionate

The quantitative determination of beclomethasone dipropionate was performed by HPLC (Agilent, USA). The HPLC system comprised a multisolvent delivery unit (Agilent 1200 series quaternary pump), an autoinjector (Agilent 1200 series, autosampler), a degasser (Agilent 1200 series, micro degasser) and a lambda absorbance detector (Agilent 1200 series, variable wavelength detector). The analysis was carried out at 40 °C using a Phenomenex Core-shell F5 column (2.6 µm, 4.6 mm x 100 mm) as stationary phase. BDP-containing solutions were isocratically eluted at a flow of 0.7 mL/min employing an acetonitrile/water (60:40 v/v) solution as mobile phase. An injection volume of 50 µL, a run time of 8 minutes and a wavelength of 254 nm were set for the analysis. The analytical method was validated in terms of linearity of the response (peak area *vs*. concentration) in the concentration range 0.11-31.75 µg/mL (LOD = 0.025 µg/mL, LOQ = 0.082 µg/mL) using mobile phase as solvent.

3.2.12 Homogeneity Test

The homogeneity of the prepared mixtures was checked at the end of the mixing procedure. For each formulation five samples (20 mg each) were collected from different spots of the powder bed. Each sample was dissolved in 50 mL of an appropriate solvent (water in the case of salbutamol sulphate, an ethanol/water 60:40 v/v solution in the case of BDP) and the quantification of the drug was performed. Homogeneity was assumed at a coefficient of variation (calculated as

the percentage of the ratio between standard deviation and mean value on the five measurements) lower than 5% (Ref EMA, 2013).

3.2.13 *In Vitro* Aerodynamic Assessment

In vitro aerodynamic assessment was performed using a Fast Screening Impactor (FSI, Copley Scientific, UK). This equipment employs two segregation stages: a Coarse Particle Mass (CFC) collecting particles with an aerodynamic diameter larger than 5 μm and Fine Particle Mass (FPM) collecting particles with an aerodynamic diameter lower than 5 μm. The FSI is composed by an Induction Port (IP), a Coarse Fraction Collector (CFC) filled with 10 mL of an appropriate solution (water for SS, methanol-water (60:40 v/v) for BDP) that acted as a liquid trap for the non-inhalable particles and by a Fine Fraction collector (FFC) fitted with a glass fibre filter (Type A/E, Pall Corporation, USA).

After completing the assembly, the FSI was connected to a VP 1000 vacuum pump (Erweka, Germany) and the flow rate through the impactor was measured by a mass flowmeter (model 3063, TSI, USA).

A medium resistance single-dose DPI, RS01® (Plastiape S.P.A., Italy), was chosen as aerosolization device. For each mixture, three Quali-V® capsules size 3 (Qualicaps® Europe, Spain) were filled with 10.0 ± 0.1 mg of powder, introduced in the inhaler device and finally pierced. Once connected the device to the impactor through an airtight rubber mouth, the vacuum pump was activated at a flow of 60 L/min for 4 seconds so that 4 L of air were drawn through the

apparatus (Ph. Eur. 8.0, 2.9.18.). Three consecutive aerosolizations were performed for each formulation. At the end of the deposition experiment, the FSI was disassembled and two different procedures were adopted depending on the API under examination. Salbutamol sulphate deposited on each stage of the impactor was recovered with aliquots of water, which were finally transferred into volumetric flasks of adequate volume and made-up to volume with water. The obtained solutions were filtered through a cellulose acetate syringe filter (porosity 0.45 µm and diameter 2.5 cm, GVS Filter Technology, USA) before being analysed. A volumetric flask was used to collect the salbutamol sulphate remained in the RS01® device and in the capsules which were dissolved in water at the end of the experiment in order to ensure complete recovery of the active ingredient. Therefore, in this case, the absorbance initially recorded was corrected by subtracting the contribution due to the absorbance of the Quali- V® capsules.

BDP was recovered from each stage of the impactor with appropriate volumes of a methanol/water 6:4 v/v solution. Before being transferred into vials, the solutions were filtered through a regenerated cellulose syringe filter (porosity 0.45 µm, diameter 2.5 cm, Analytical Technology, Italy).

All the mixtures were tested in triplicate immediately after preparation. Their performance was evaluated by calculating:

- emitted dose (ED), obtained as the sum of the portions of drug recovered from the induction port, the CFC stage and FFC stage expressed in µg;

- fine particle dose (FPD), namely the quantity of drug with a cut-off diameter lower than 5 μm, calculated by interpolation according to the European Pharmacopoeia (Ph. Eur. 8.0, 2.9.18.) and expressed in μg;
- the fine particle fraction (FPF), calculated as the ratio of the FPD to the ED expressed as percentage.

3.2.14 Powder Dry dispersion

The dry dispersion of the powder was performed using the QicPic DIA apparatus equipped with RODOS (Sympatec Inc., Clausthal-Zellerfeld, Germany). Dry powders were fed into the high-speed dry-sample disperser where they were accelerated via a Venturi tube located in the dispersing line. During this process, dry powders were dispersed and aerosolized by particle–particle, particle–wall collisions and centrifugal forces caused by velocity gradients. The process was controlled by Windox software (Sympatec Inc., Clausthal-Zellerfeld, Germany).

Sympatec QicPic/RODOS was operated at different pressures ranging from 0.1 bar to 1.2 bar, to investigate the de-aggregation of the carrier granules. Furthermore, the relative mechanical strength of different agglomerate was evaluated by comparison of the fraction of particles less than 150 μm, obtained at different pressures. The cut off value of 150 μm was chosen considering the particle size of LH100 raw material (Dv50 125-150 μm). To study the agglomerate strength, the fraction <150 μm was used as a measure reflecting how the agglomerates were broken at different pressure. Two repeated measurements were carried out at all pressures for each carrier sample.

For every QicPic/RODOS measurement approximately 0.7 g of powder was used. To minimize the sampling error the tested powder was automatically subdivided with a sample divider Laborette 27 (Fritsch GmBH, Germany).

3.2.15 Specific surface area

The specific surface area of the carriers was investigated using the Micromeritics Tristar II 3020 (Norcross, USA). All samples were vacuum dried for two days at 25°C using the Micromeritics VacPrep 061 degas unit (Norcross, USA). The measurements were performed using nitrogen adsorption and desorption isotherms at the temperature of liquid N_2 (-196 °C); Brunauer, Emmett, and Teller (BET) (Emmett, 1936) adsorption theory was used to calculate the specific surface area, using a pressure range of 0.05–0.30 normalized to the saturation pressure of the adsorbate. 1.5 g of powder was used, resulting in BET correlation factors above 0.999, indicating applicability of the method. Each measurement was carried out in triplicate.

3.2.16 Powder flowability

Powder flowability was performed using a FT4 powder rheometer (Freeman Technology, UK) (Freeman, 2007). In this study, powder flowability was investigated using the powder rheometer in the dynamic mode. In dynamic mode, a blade with a diameter of 23.5 mm was traversed through the 25 ml samples in a 25 mm diameter borosilicate glass vessel with a blade tip speed of 100mm/s and a helix angle of −5°. The energy (mJ) required to move the blade

through the powder during a downward traverse namely from the top to the bottom of the vessel was defined as basic flowability energy (BFE). Furthermore, the specific energy (SE) that is the energy (mJ) per gram established on the upward traverse, was measured; in this case the powder was unconfined (powder can lift up) and so the energies measured were more depending on the cohesive and mechanical interlocking forces between the particles and less influenced by other factors such as the compressibility that can be very significant in the BFE test.

All samples before the measurement were pre-conditioned using the instrument's 'conditioning' process. The 'conditioning' blade action gently disturbs the powder bed and creates a uniform and slightly packed test sample in order to remove any pre-compaction and excess of air from the sample.

3.2.17 Contact angle

The contact angles of the samples were measured applying the Wilhelmy plate technique (Ramé, 1997), using a Tensiometer K12 (Krüss GmbH, Germany).

For this purpose, a 20x20 mm double-sided adhesive tape was used and completely covered with the tested powder. The solid sample was hung perpendicular to the liquid surface. Three different liquids were used, two polar (water and ethylene glycol) and one non-polar (di-iodomethane). Each liquid was placed in a clean glass dish and raised by means of a motorized platform to contact the powder plate. The platform was raised at the speed of 6 mm/min

and the submersion distance was 2 mm. The volume of liquid used for the contact-angle measurements was ca. 50 mL. The contact angle was calculated from the measured force by transposing the Wilhelmy equation using Krüss Laboratory Desktop Software (Krüss GmbH, Germany).

3.2.18 Surface energy

The solid´s surface free energy was calculated using the Good and van Oss method for contact angle using the above mentioned three liquids having known non-polar (γ^{LW}), acid (γ^{+}) and base (γ^{-}) components. The total energy, which is the sum of the non-polar (LW, Lifshitz-van der Waals) and polar (AB, acid-base) components, is given by equation 3 (Van Oss et al., 1988):

$$(1 + \cos\theta)\gamma_l^{TOT} = 2\left(\sqrt{\gamma_S^{LW}\gamma_l^{LW}} + \sqrt{\gamma_S^{+}\gamma_l^{-}} + \sqrt{\gamma_S^{-}\gamma_l^{+}}\right) \quad \text{(Equation 3)}$$

where θ is the contact angle value between solid and liquid, γ_l^{TOT} the surface tension of test liquid, γ_S^{LW} and γ_l^{LW} are the non polar component of surface energy for the tested solid and liquid, respectvily, while γ_s^{+}, γ_s^{-}, γ_l^{+}, and γ_l^{-} are the polar component for the surface energy of the tested solid and liquid, respectively.

The system of linear equations was solved using R version 3.2.1 (general public license software, Matlab) and liquids surface tension parameters defined by Van Oss (Van Oss et al., 1997).

3.2.19 Work of adhesion and cohesion

The work of cohesion (equation 4) (W^{coh}) between the API particles and the work of adhesion (equation 5) (W^{adh}) between drug and carrier was determined by using the computed components for the surface energy of the solids according to Young-Dupré (Schrader, 1995):

$$W_{ii}^{coh} = 2\gamma_{ii} \quad \text{(Equation 4)}$$

$$W_{ij}^{adh} = \gamma_i + \gamma_j - \gamma_{ij} \quad \text{(Equation 5)}$$

where γ_i and γ_j are the surface energies of the tested interacting materials and γ_{ij} the interfacial energy of their surfaces.

The interfacial energy γ_{ij} was calculated by using van Oss, Chaudhury, and Good method (Biresaw & Carriere, 2001) as describe in the following Equation 6:

$$\gamma_{SP}^{TOT} = [\sqrt{\gamma_S^{LW}} - \sqrt{\gamma_P^{LW}}]^2 + 2[\sqrt{\gamma_S^+\gamma_S^-} + \sqrt{\gamma_P^+\gamma_P^-} - \sqrt{\gamma_S^+\gamma_P^-} - \sqrt{\gamma_S^-\gamma_P^+}] \quad \text{eq. (6)}$$

4 Results and Discussion

4.1 Lactose characterization

The starting materials Lactohale LH100, Respitose ML006 and Inhalac 50 were characterized with different techniques in order to evaluate the physico-chemical properties of these materials.

4.1.1 Differential Scanning Calorimetry (DSC)

The solid state of the starting materials was evaluated using the DSC. Figure 12 shows the DSC traces of the reference lactose samples.

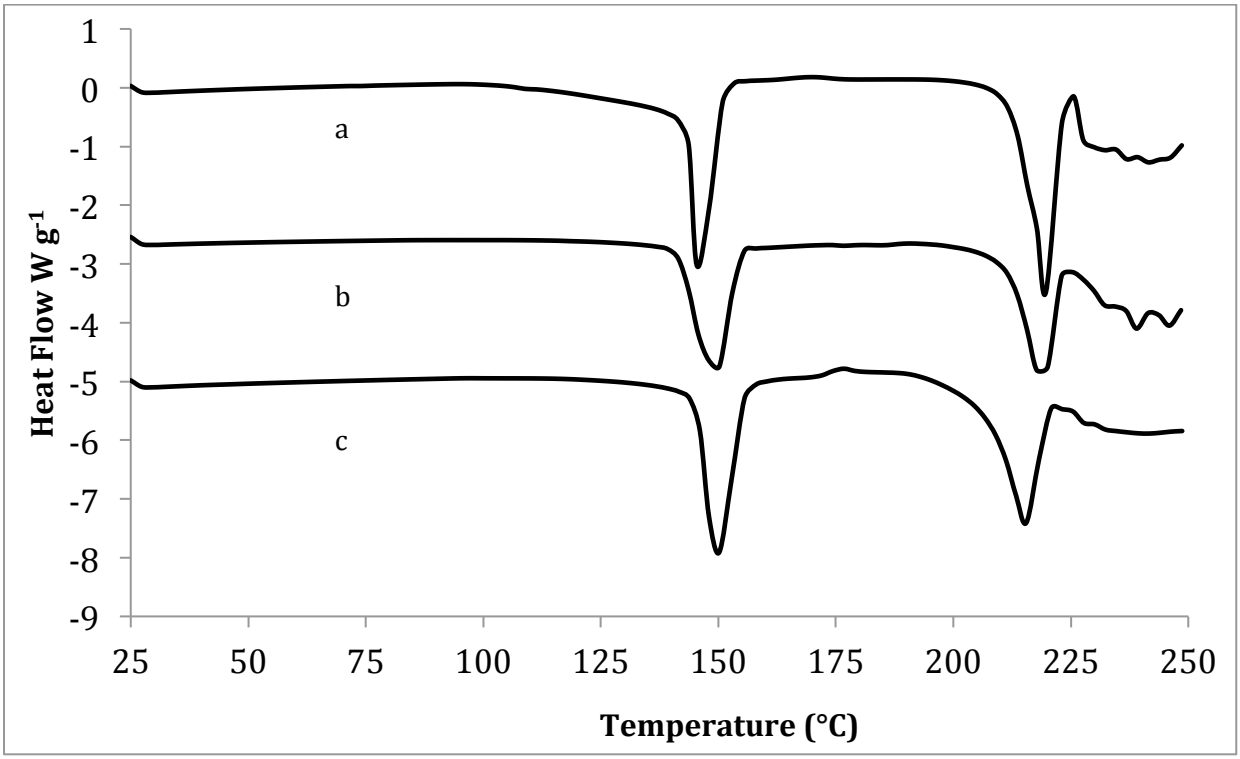

Figure 12 DSC traces of: a) Respitose ML006; b) Inhalac 50; c) Lactohale LH100.

The DSC traces of Respitose ML006 and Inhalac 50 showed a typical lactose monohydrate behaviour with an endothermic peak respectively at 146.0 °C and 149.5 caused by the evaporation of the water of crystallization and a second endothermic peak respectively at 219.7 and 218.9 corresponding to the melting of lactose before decomposition (Listiohadi & Hourigan, 2009)(Della Bella et al., 2016). Similarly to the previous two, the DSC trace of Lactohale LH100 showed a monohydrate behaviour with an endothermic peak at 149.8 °C and a second endothermic peak at 215.5 °C, but differently by the other two raw materials it showed a slight exothermic peak at 176.1 that could be ascribed either to recrystallization of lactose distortions, that is the conversion of amorphous lactose to crystal (Figura, 1993),(Gombás et al., 2002) or to the recrystallization following the melting of a small portion of a metastable anhydrous α-lactose (Della Bella et al., 2016).

Solid State characterization with DSC was performed on lactose samples obtained with the *Procedure #1* (Microwave preparation of lactose powder using water as binder solution) (Figure 13) in order to evaluate if the microwave drying process and the addition of the water, as binder, would have led to changes of the physico-chemical characteristics of the treated lactose.

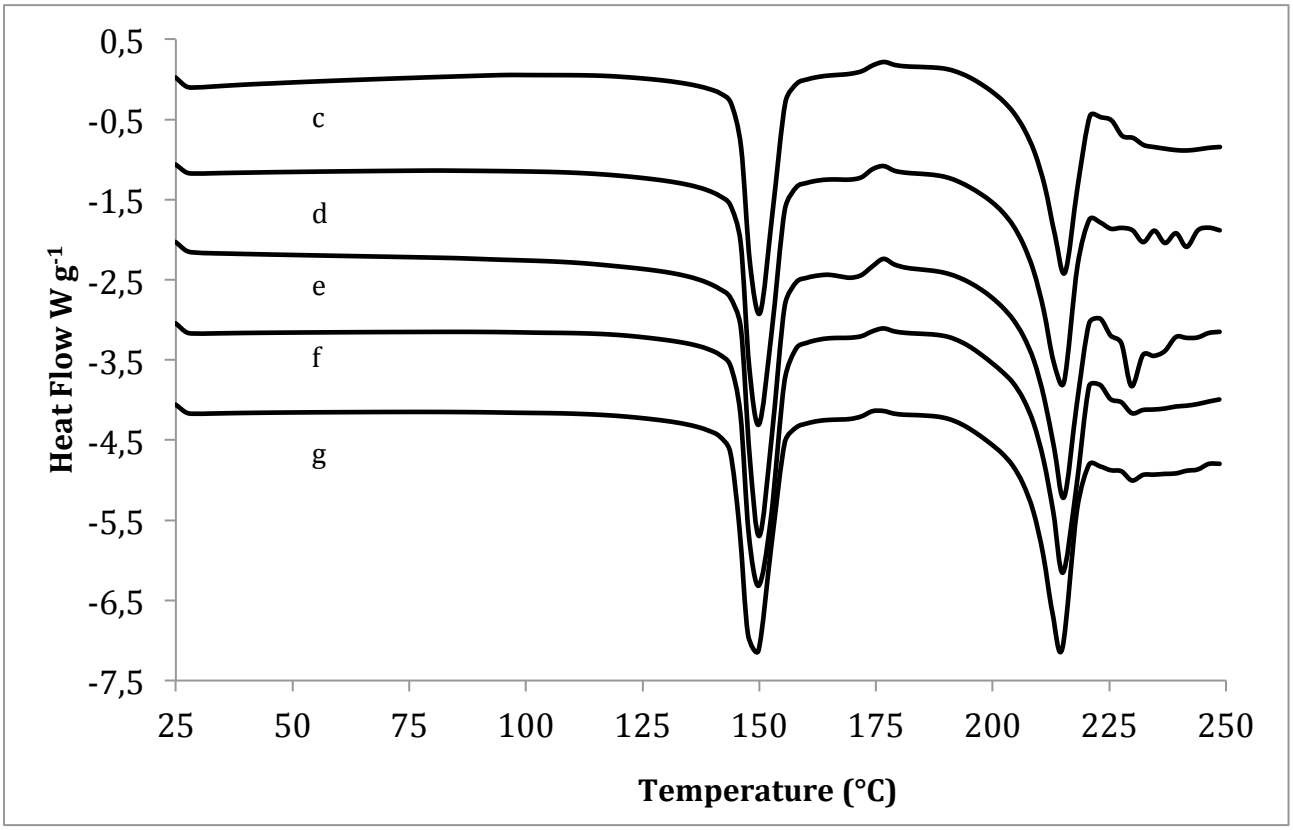

Figure 13 DSC trace of: c) Lactohale LH100 raw material; d) Lactohale LH100 prepared with 5% of water; e) Lactohale LH100 prepared with 10 % of water; f) Lactohale LH100 prepared with 15% of water; g) Lactohale LH100 prepared with 20% of water.

As can be appreciated in the Figure 13 that all traces afforded the two endothermic peaks and the exothermic peak detected in the DSC trace of Lactohale LH100 raw material. Therefore, it can be stated that neither the addition of water in different amount (from 5% to 20%) as a binder solution nor the drying microwave process created changes in the solid state of Lactohale LH100.

A further DSC investigation was conducted on lactose samples after the *Procedure #2* (Microwave preparation of lactose granules using an almost saturated lactose solution as binder).

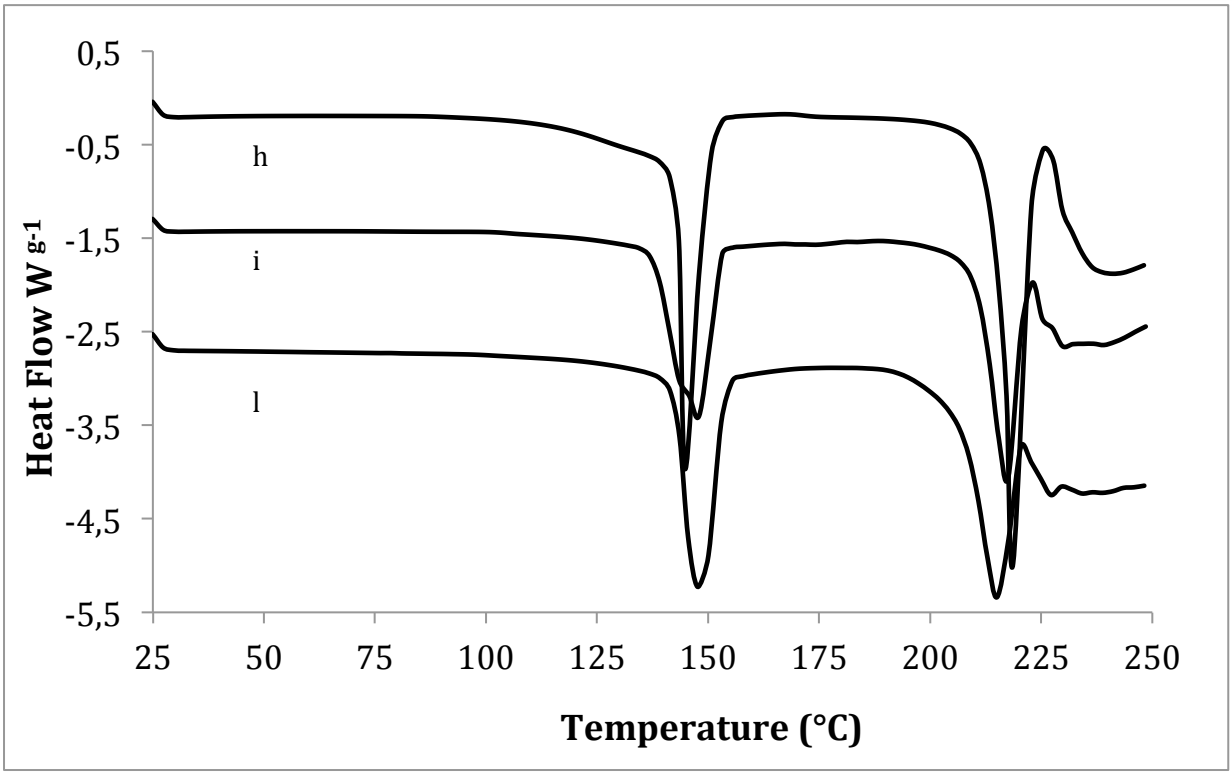

Figure 14 h) DSC trace of Respitose ML006 prepared with 15 % of almost saturated lactose solution dried at microwave; i) DSC trace of Inhalac 50 prepared with 15 % of almost saturated lactose solution dried at microwave; l) DSC trace of Lactohale LH100 prepared with 15 % of almost saturated lactose solution dried at microwave.

Figure 14 shows the traces of the three lactose powders treated with the *Procedure #2*; Respitose ML006 (h) and Inhalac 50 (i) traces highlighted the first endothermic peak due to water of crystallization and the second peak caused by the melting of lactose as was observed in the respectively raw material DSC traces (Figure 3 traces a and b). As regards the Lactohale LH100 DSC trace (l) after the *Procedure* #2 a difference with the raw material trace was noted; although the two endothermic peaks are present, the exothermic peak around 175 °C was lacking. This behaviour could be explained considering the different microwave drying process; since, unlike the *Procedure #1* where the samples were dried at 250 W for 5 minutes in the case of *Procedure #2* the samples were dried at 600W for five minutes. The lack of the exothermic can be hardly

ascribed to the binder solution because the only difference in the binder solutions used in the *Procedure #1* compared to the solution used in the *Procedure #2* is the lactose used to prepare the almost saturated lactose solution that is lactose Lactohale LH100 in the case of sample prepared starting from Lactohale LH100.

4.1.2 Thermo gravimetric analysis (TGA)

TGA were performed on the three raw materials Lactohale LH100, Respitose ML006 and Inhalac50 and confirmed the thermal behaviour reported in the DSC results; indeed, in the Figures 15-16-17 it is possible to appreciate a first step (weight loss around 5%) that corresponds to the evaporation of the water of crystallization followed by a step relevant to the lactose decomposition.

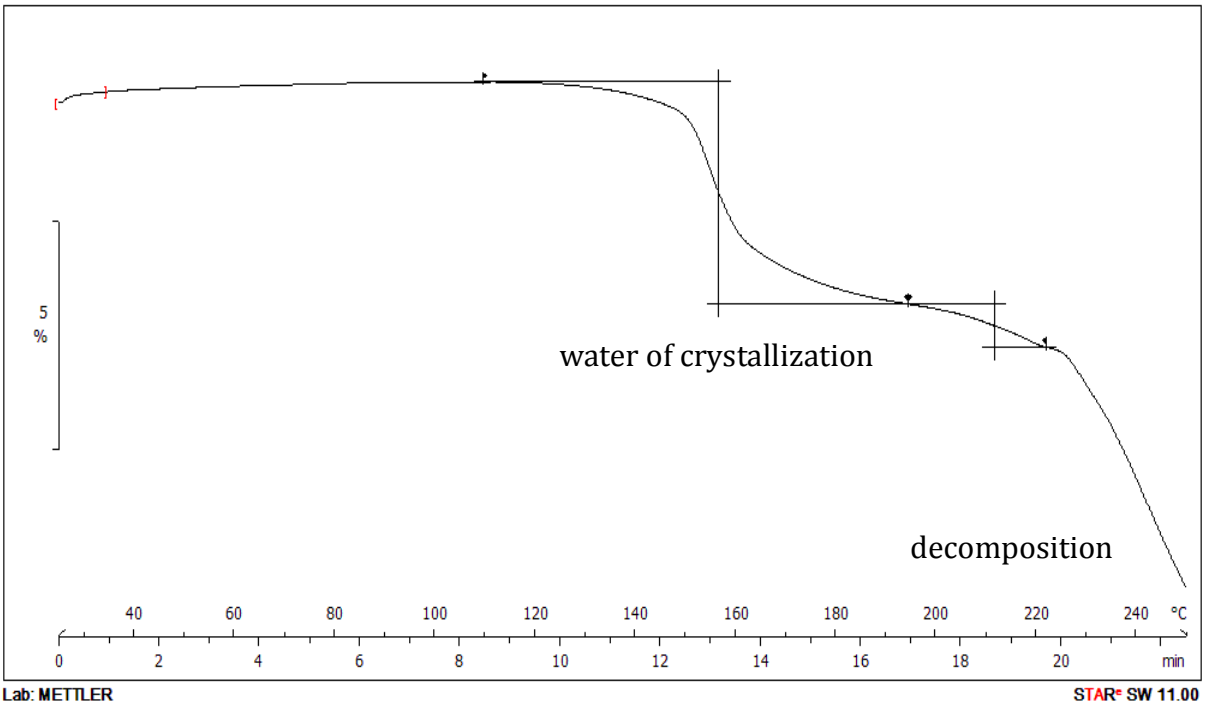

Figure 15 TGA trace of Lactohale LH100 raw material.

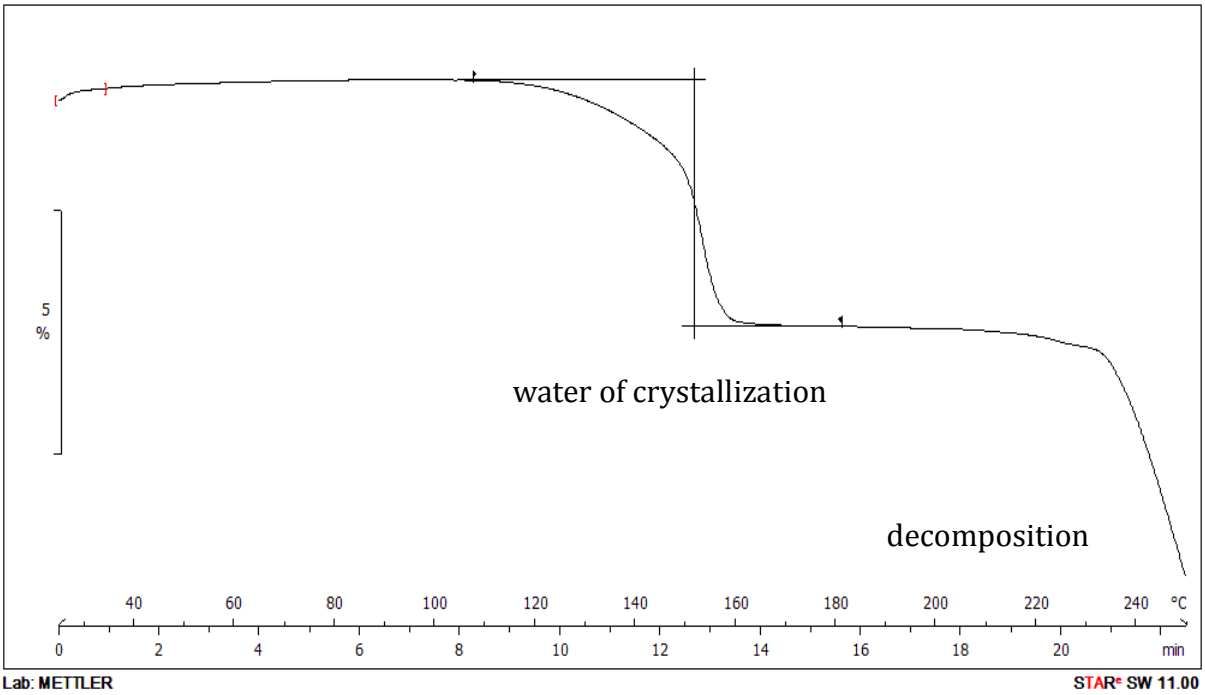

Figure 16 TGA trace of Respitose ML006 raw material.

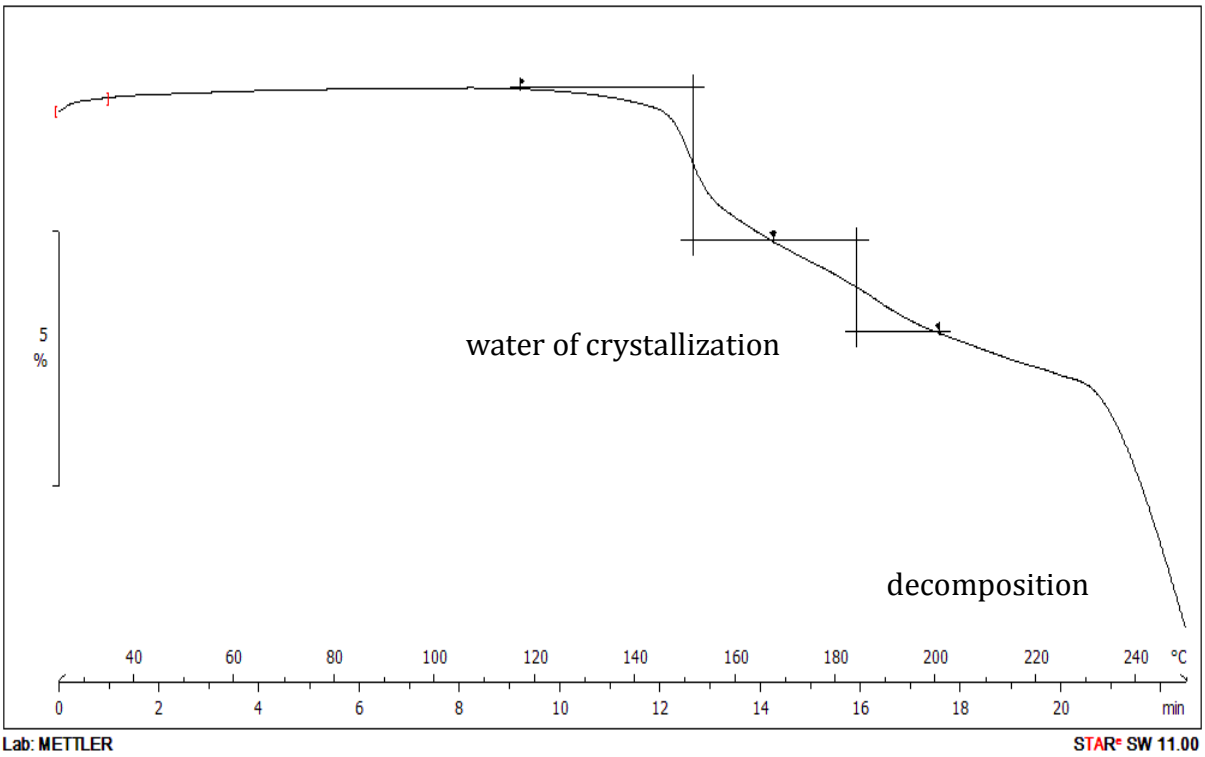

Figure 17 TGA trace of Inhalac 50 raw material.

4.2 Procedure #1: Microwave preparation of lactose granules using water as binder solution

As a first approach Lactose Lactohale LH100 was wetted with an increasing amount of water (5, 10, 15 and 20%) used as binder. The purpose was to assess the suitable amount of liquid in order to obtain a slurry while not dissolving the lactose in order to avoid the formation of amorphous material during the drying process.

After the samples production, a dimensional analysis with sieves was performed to investigate the particle size of the carriers in order to figure out what was the most suitable amount of water to use in the process.

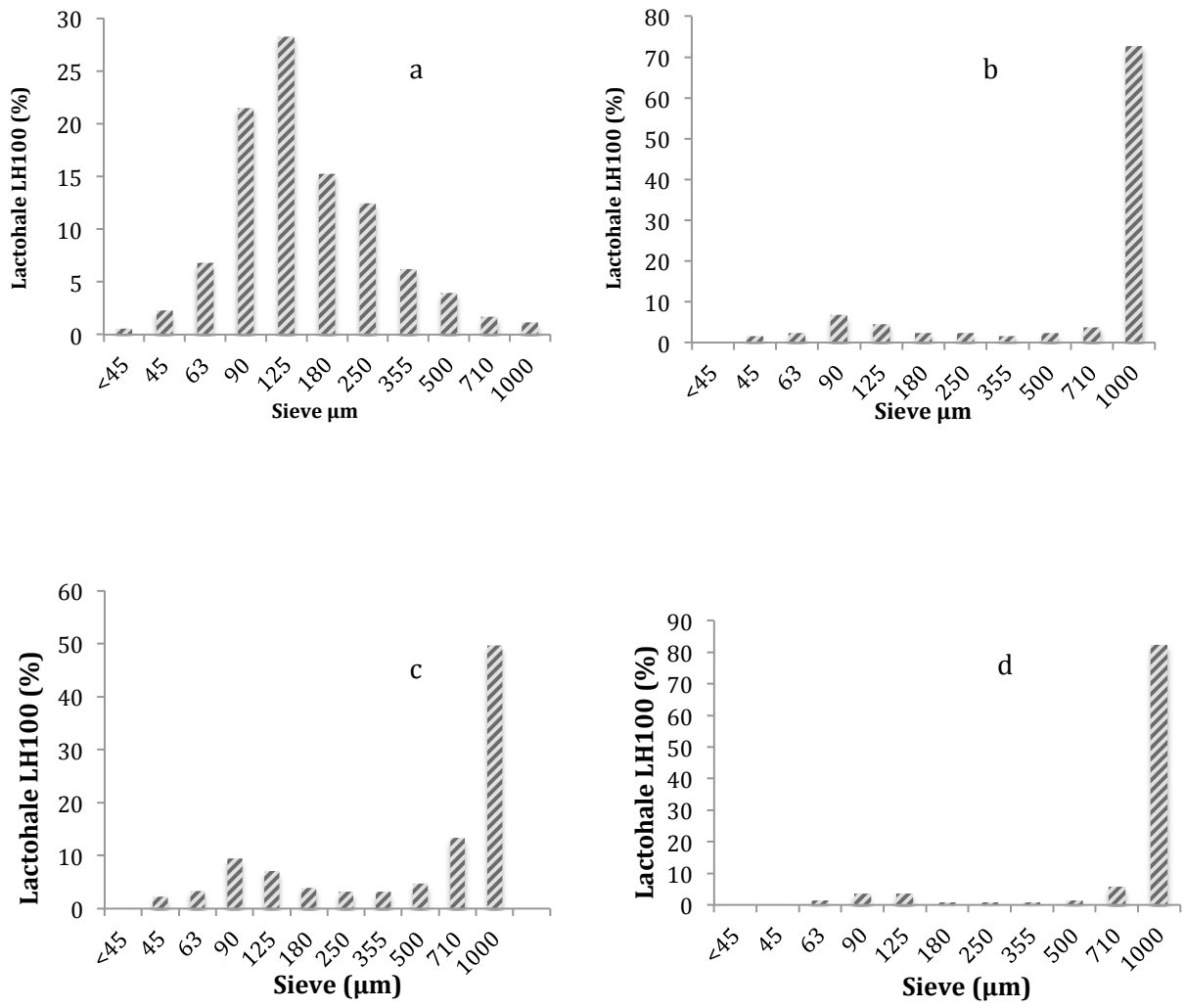

Figure 18 a) Size distribution of Lactohale LH100 prepared with 5 % of water; b) size distribution of Lactohale LH100 preapred with 10 % of water; c) size distribution of Lactohale LH100 prepared with 15 % of water; d) size distribution of Lactohale LH100 prepared with 20 % of water.

Figure 18 shows the size distribution of the carriers produced with an increasing amount of water; lactose powder produced with 5 % of water presents the same particle size distribution of the raw material (data not shown) and this can be ascribed to the limited water amount used as a binder and to the low microwave power (250 W). On contrary, the addition of a percentage of water higher than 5% w/w leads to the formation of strong and big aggregates (Figure 18, b, c and d). This phenomenon can be explained by the lofty water

content that creates a large amount of bridges among the lactose particles as well as by the significant heating stemming from the larger amount of solvent with high dielectric component.

To better investigate the suitable parameter to customize a carrier, a Design of Experiment (DoE) was constructed.

Table 2 and 3 illustrate the results of a fractional factorial design with central point conducted on Respitose ML006 and Lactohale LH100 respectively.

Table 2 DoE parameters and results using Respitose ML006

	Input variables			Output variables		
	Power (W)	Water (% w/w)	Time (min)	Yield (%) >180 µm	Friability (%)	% Water
#1	250	15	10	25.12	23.47	0
#2	250	15	10	31.31	80.33	0
#3	600	15	5	66.84	84.86	0
#4	600	15	5	45.18	80.46	0
#5	250	25	5	0[2]	100	9.05
#6	250	25	5	0[2]	100	9.5
#7	600	25	10	6.15	54.55	0
#8	600	25	10	8.76	38.89	0
#9	425	20	7.5	41.12	74.68	0
#10	425	20	7.5	32.14	22.13	0

[2] The powder was too wet to pass through the 180µm sieve

Table 3 Doe parameters and results using Lactohale LH100

	Input variables			Output variables		
	Power (W)	Water (%w/w)	Time (min)	Yield (%) <180 µm	Friability (%)	% Water
#1	250	15	10	26.02	49.02	0.1
#2	250	15	10	31.31	80.33	0.1
#3	600	15	5	15.81	6.67	0
#4	600	15	5	20.51	43.69	0
#5	250	25	5	0[3]	100	13.30
#6	250	25	5	0[3]	100	15.01
#7	600	25	10	6.31	69.24	0
#8	600	25	10	64.66	63.66	0
#9	425	20	7,5	32.00	32	0
#10	425	20	7,5	46.57	46.57	0

The outcome results for both Respitose ML006 and Lactohale LH100 showed a very high friability except the sample#3 for Lactohale LH100 that showed a value around 7%. As it can be appreciated in the Table 4 and 5 that describe the statistical significance of the results for Respitose ML006 and Lactohale LH100 respectively, the amount of water add had the most significant negative influence on the yield. On the other hand, all the three input parameters showed a very significant effect on the residual moisture of the prepared powders: as expected the power and treatment time exerted a negative effect (more dry lactose samples), while the amount of water added afforded a significantly more wet powders.

[3] The powder was too wet to pass through the 180µm sieve

Table 4 Respitose ML006 significance of the results. NS = non-significant; + or - = 95% probability positive or negative influence; ++ or -- between 95 and 99% probability positive or negative influence; +++ or ---probability higher than 99% positive or negative influence.

	Yield (%) >180 µm	Friability (%)	% Water
Power (W)	+	NS	---
Water added (%)	--	NS	+++
Time (min)	NS	-	---

Table 5 Lactohale LH100 significance of the results. NS = non-significant; + or - = 95% probability positive or negative influence; ++ or -- between 95 and 99% probability positive or negative influence; +++ or --- probability higher than 99% positive or negative influence.

	Yield (%) >180 µm	Friability (%)	% Water
Power (W)	NS	-	---
Water added (%)	---	+	+++
Time (min)	+	NS	---

As sample #3 of Lactohale LH100 (Table 3) showed the most suitable properties in particular with respect to friability (particle size of the sample remaining almost unchanged upon mechanical stress), the conditions used form its preparation were selected for producing the carriers used in further investigation.

4.3 Procedure #2: Microwave preparation of lactose granules using an almost saturated lactose solution as binder

4.3.1 Respitose ML006 and Lactohale LH100 granules investigation

As the friability of the samples produced with Procedure #1 was in all cases too high, water was substituted with an almost saturated lactose solution as binder.

4.3.1.1 Samples Friability

The friability test carried out on samples forced to a 425 μm and 212 μm sieve had a friability of 0% and 33% respectively. The friability outcomes indicate that the almost saturated lactose solution used as a binder increased the granules strength. This behaviour is due to the fact that the lactose in the solution creates bridges between the lactose particles during dried thus, increasing the granules hardness.

4.3.1.2 Scanning electron microscopy

Figures 19 and 20 show the SEM pictures of Lactohale LH100 forced through 425 μm and 212 μm sieve respectively while Figures 21 and 22 show the SEM pictures of Respitose ML006 forced through the same sieves. The pictures on the left-hand side show a panoramic view of the lactose population while the pictures on the right-hand side show the granules detail. It can be noted that the lactose aggregates of Lactohale LH100 (Figure 19-20) exhibited large inter-

particles spaces due the greater particle size of the starting material (dv50 = 125 µm) compared to of Respitose granules (Figure 21-22) that show a more compact structure with narrower and less deep inter-particles spaces (Respitose ML006 dv50 = 17 µm).

All the four prepared carried presented interesting physical and morphological features for further development of drug-carrier mixture. Therefore they were used to prepare binary mixture with the two model drugs.

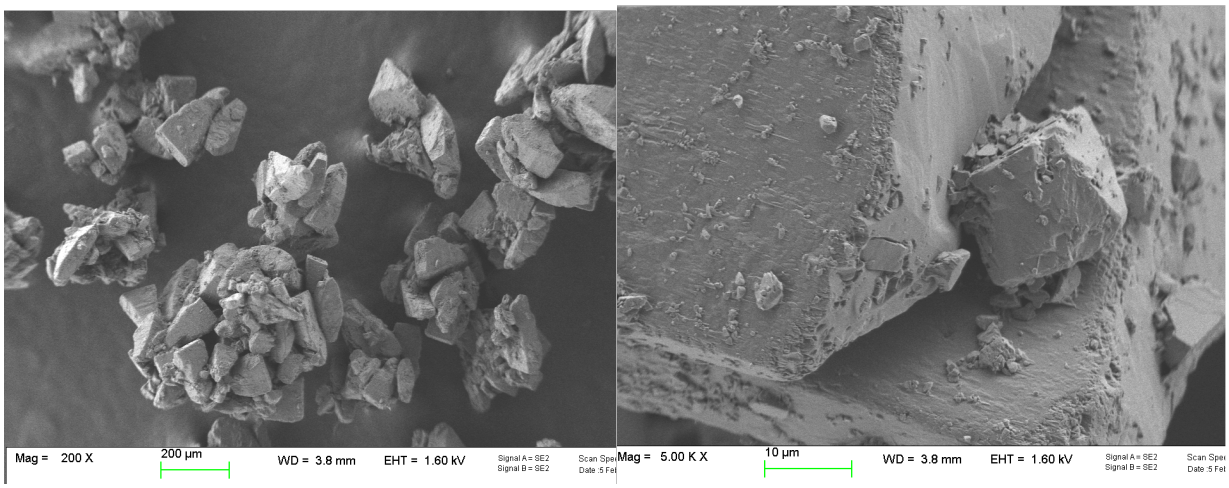

Figure 19 Pictures of Lactose Lactohale 100 at 200X (left) and 5000X (right) prepared with 15% almost saturated lactose aqueous solution sieved through **425 µm.**

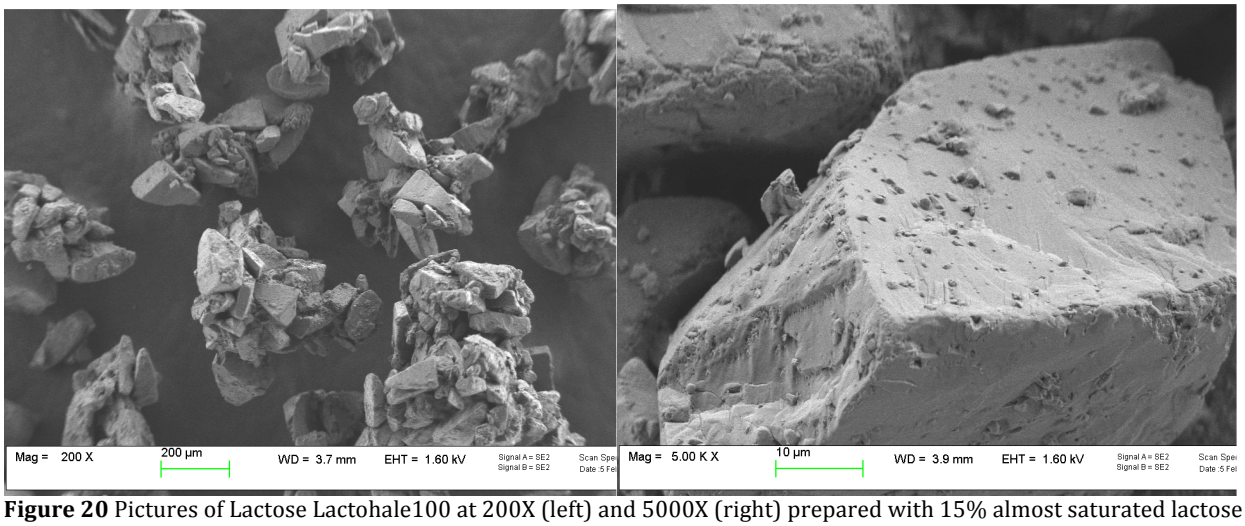

Figure 20 Pictures of Lactose Lactohale100 at 200X (left) and 5000X (right) prepared with 15% almost saturated lactose aqueous solution sieved through **212 µm.**

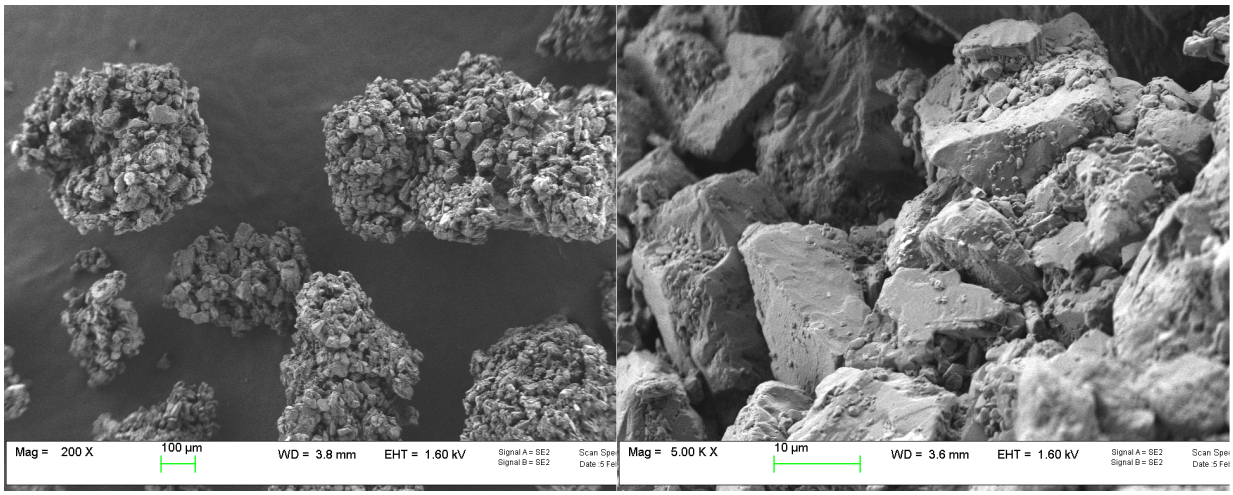

Figure 21 Pictures of Lactose Respitose at 200X (left) and 5000X (right) prepared with 15% almost saturated lactose aqueous solution sieved through **425 µm.**

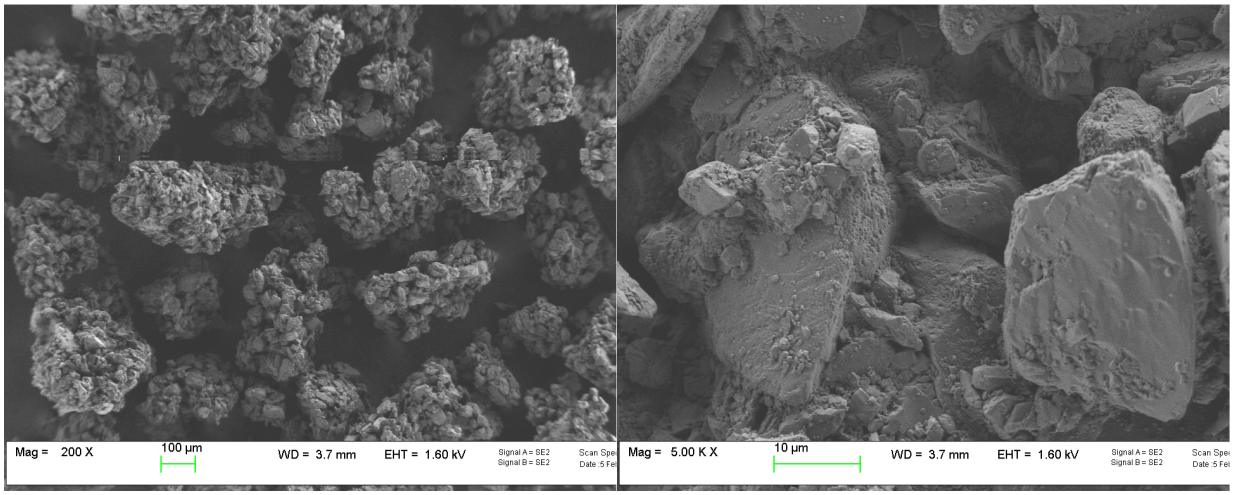

Figure 22 Pictures of Lactose Respitose at 200X (left) and 5000X (right) prepared with 15% almost saturated lactose aqueous solution sieved through 212 µm.

4.3.2 Assay and content uniformity

Content uniformity test on Lactohale LH100, Respitose ML006 and Inhalac 50 was performed; both raw material and granules samples were evaluated.

Table 6 shows the uniformity content of BDP and SS blends; BDP and SS were successfully blended with lactose LH100 and Inhalac 50 granules. The same did not occur with Respitose that gave rise to slightly higher variability of drug content in particular for the batch #4 and #6, that close to the acceptable value

according to the EMA guideline (RDS≤ 5%). Considering the morphological differences between the Lactohale-LH100 and Respitose-containing granules (Figures 19-22), it can be speculated that the poorer miscibility observed with the latter can be ascribed to the smaller dimension of the inter-particle spaces that were likely less prone to receive and allocate in a homogeneous manner the micronized BDP particles.

Table 6 Drug content ± standard deviation and uniformity of BDP and SS blends.

batch		BDP µg/10 mg blend	RSD %
#1	**BDP/LH100 raw material**	94.6 ± 2.09	2.14
#2	**BDP/LH100 212 µm**	98.7 ± 0.99	1.01
#3	**BDP/LH100 425 µm**	93.4 ± 2.09	3.62
#4	**BDP/Respitose raw material**	93.5 ± 4.79	5.12
#5	**BDP/Respitose 212 µm**	86.6 ± 1.71	1.98
#6	**BDP/Respitose 425 µm**	95.2 ± 4.62	4.85
#7	**SS/LH100 raw material**	86.4 ± 2.77	3.22
#8	**SS/LH100 212 µm**	99.0 ± 2.31	2.33
#9	**SS/LH100 425 µm**	97.6 ± 0.70	0.71
#10	**BDP/Inhalac raw material**	65.6 ± 2.5	3.82
#11	**BDP/Inhalac 425 µm**	96.1± 4.4	4.56
#12	**SS/Inhalac raw material**	101.8 ± 3.0	2.98
#13	**SS/Inhalac 425 µm**	97.6 ± 0.7	0.71
#14	**BDP/425 µm LH100 granules***	98.7 ± 1.6	1.66
#15	**SS/425 µm LH100 granules***	86.4 ± 2.8	3.22

*Prepared with raw material having particle size > 125µm

4.3.2.1 In vitro aerosolization of lactose-BDP and lactose-SS blends

The Fast Screening Impactor was adopted for the determination of the aerodynamic size distribution of the aerosolized.

The results obtained for each formulation are summarized in Table 7 as Emitted Dose (ED), Fine Particle Dose (FPD) and Fine Particle Fraction (FPF). The illustrated data are the average of three tests carried out in three different days (9 capsules in total).

The Lactohale-BDP blends presented an ED higher than that of the raw the blend prepared with the same drug and the raw material. In the case of SS the ED increased only with Lactohale 212 μm granules compared to the raw material blend. As regards to the FPF of the BDP blends, in the case of Lactohale, it duplicated (12.9 %) and triplicated (18.0 %) in the batch #2 and #3 respectively compared to BDP/raw material blend (#1, 5.4 %). As opposed Respitose granules did not provide an increase of performance, in particular, BDP/Respitose raw material blend (#4) exhibited and high FPF (25.6 %) that was equalled when BDP was blended with respitose 425 μm granules (24.7 %, #6) but became lower when BDP was blended with a Respitose 212 μm granules (#5, 14.1 %).

SS showed a significant increase of respirability when it was blended with LH100 granules with respect to the raw material. Moreover, the comparison between the respirability of SS and BDP, with the same carrier, suggests that the

hydrophilic molecule detached more easily from the surface of the lactose surface compared to the more hydrophobic. In detail, the fine particle fraction of the blends prepared with the granules compared to the LH100 raw material blend, increased significantly form 31.87 % (#7) to 47.02% (#8) and 39.39 % (#9) when the LH100 212 μm granules and 425 μm granules respectively were employed.

As far as the Inhalac material is concerned, the emitted doses obtained for both tested API slightly increases when drugs were blended with granules compared with raw material. In particular the emitted dose increased from 43.2 μg to 53.2 μg for BDP and from 72.1 μm to 87.1 μm for SS. As regards the fine particle fraction Inhalac 425 μm granules equalized the results obtained with the raw material for both drugs.

Furthermore, also the mixture obtained with the LH100 425 μm granules prepared with lactose having a particle size higher than 125 μm, afforded an aerodynamic performance comparable to that of the mixture prepared with the "normal" LH100 425 μm granules, indicating that the elimination of the fine component of lactose before the granules preparation did not exert a positive effect on the granules performance when used as carrier.

Is possible to conclude that Lactohale LH100 granules increase the drug detachment in particular with the granules of bigger dimension, in particular for BDP.

Table 7 Emitted Dose, Fine Particle dose and Fine Particle Fraction ± standard deviation of BDP and SS blends prepared with LH and Respitose raw material or granules.

Batch		ED (µg)	FPD (µg)	FPF (%)
#1	**BDP/LH100 raw material**	45.9 ± 6.7	5.4 ±1.2	5.4 ± 0.9
#2	**BDP/LH100 212 µm**	66.9 ± 25.4	11.7± 2.0	12.9 ± 1.1
#3	**BDP/LH100 425 µm**	56.16 ± 15.2	14.9 ± 4.0	18.0 ± 1.3
#4	**BDP/Respitose raw material**	54.1 ± 23.9	21.6 ± 7.6	25.6 ± 5.3
#5	**BDP/Respitose 212 µm**	45.43 ± 52.3	12.4 ± 1.8	14.1 ± 4.8
#6	**BDP/Respitose 425 µm**	63.8 ± 49.0	22.0 ±2.8	24.7 ± 2.1
#7	**SS/LH100 raw material**	139.6 ± 9.5	84.6 ± 6.1	31.9 ± 1.2
#8	**SS/LH100 212 µm**	180.5± 33.6	103.2 ± 14.1	47.0 ± 2.44
#9	**SS/LH100 425 µm**	143.8 ± 8.7	92.0 ± 4.3	39.4 ± 1.1
#10	**BDP/Inhalac raw material**	43.2 ± 14.9	6.7 ± 1.2	11.7 ± 2.5
#11	**BDP/Inhalac 425 µm**	53.2 ± 7.2	11.3 ± 0.3	10.4 ± 0.3
#12	**SS/Inhalac raw material**	72.1 ± 42.7	27.1 ± 2.1	26.8 ± 7.9
#13	**SS/Inhalac 425 µm**	87.1 ± 42.5	22.45 ± 2.8	27.34 ± 4.0
#14	**BDP/425 µm LH100 granules****	62.5± 5.0	12.1 ± 2.1	13.6 ± 2.7
#15	**SS/425 µm LH100 granules****	92.17 ± 23.0	48.13 ±0.6	39.1 ± 1.4

*Capsules filled with 20 mg of blend instead of 10 mg
** Prepared with raw material having particle size > 125µm

4.3.3 Proton Nuclear Magnetic Resonance (^{1}H-NMR)

The anomeric composition of each lactose sample was determined through ^{1}H NMR by applying the method described by Jawad et al. (2012).

The analysis was performed on lactose raw material as well on the three types of lactose granules obtained by microwave drying using an almost saturated lactose solution as binder. The tested granules those obtained by forcing the slurry through a 425 μm sieve.

List of samples analysed:

- Lactohale LH100 raw material;
- Respitose raw material;
- Inhalac 50 raw material;
- Lactohale LH100 425 μm granules;
- Respitose 425 μm granules;
- Inhalac 50 425 μm granules.

As an example, Figure 23 shows the pattern of LH100 raw material where the first peak on the left-hand side corresponds to the signal of β-lactose and the second peak, on the left-hand side, corresponds to the signal of α-lactose. The ratio between the two peaks was used to quantify the anomeric composition of each sample.

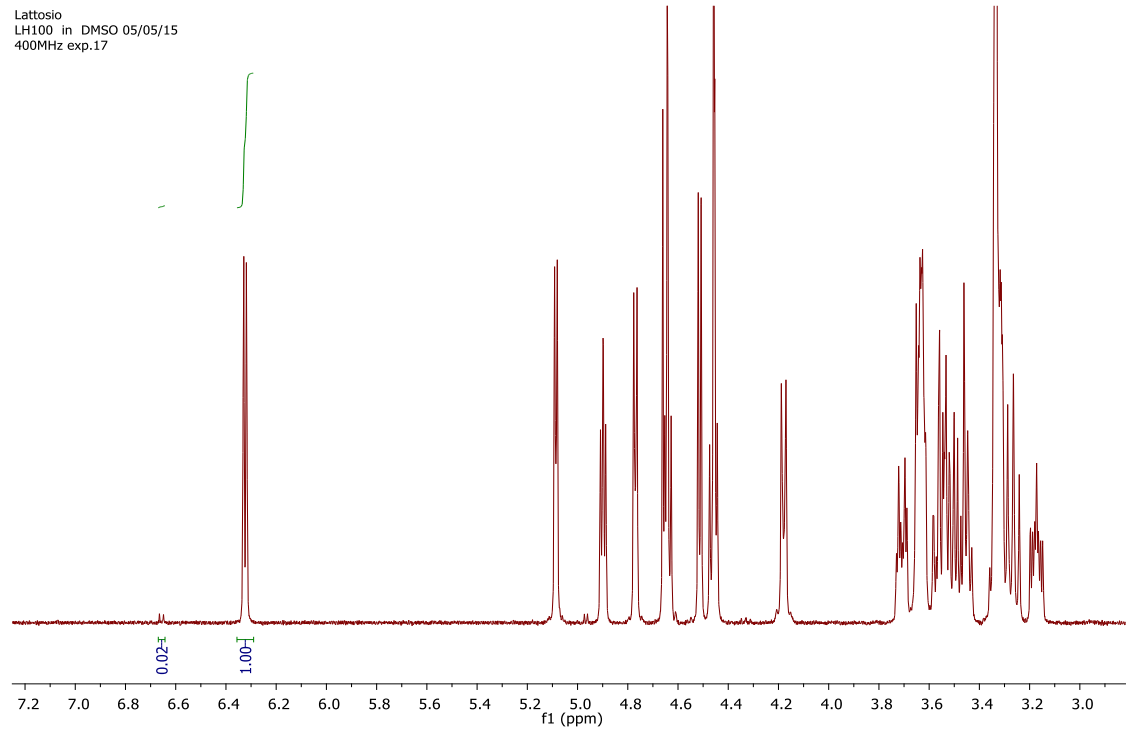

Figure 23 ^{1}H-NMR spectrum of Lactohale LH100 raw material.

Lactose in solution at the equilibrium exists for 64% in β-lactose and for 36% in α-lactose (Della Bella et al., 2016). Hence, it was calculated that, according to the amount of almost saturated solution used to prepare the slurry, a 3.2% w/w of β-lactose was added each time to the lactose raw material treated with microwave.

The β-lactose content measured in each raw material, as well as in the granules obtained after microwave treatment is reported in Table 8.

Thus, the percentage of β-lactose generated as a consequence of the granules production (%βGranules) was calculated as:

$$\%\beta Granules = \%\beta Samples - \%\beta RawMaterial - 3.2$$

(equation 7)

where %βsample and %βRawMaterial were the percentage of β lactose measured in the granules and in the starting raw material respectively.

Table 8 β content in percentage in lactose raw materials and lactose carriers treated with microwave (MW).

	β-lactose in the granules	β-lactose generated in the process of granules production (%)
Respitose raw material	3.02	
Respitose MW	10.92	4.7
LH100 raw material	1.46	
LH100 MW	6.07	1.41
Inhalac raw material	2.73	
Inhalac MW	5.13	0

It is interesting to note that the amount of β lactose generated by the granules production was inversely related to the particle size of the raw material (Figure 24).

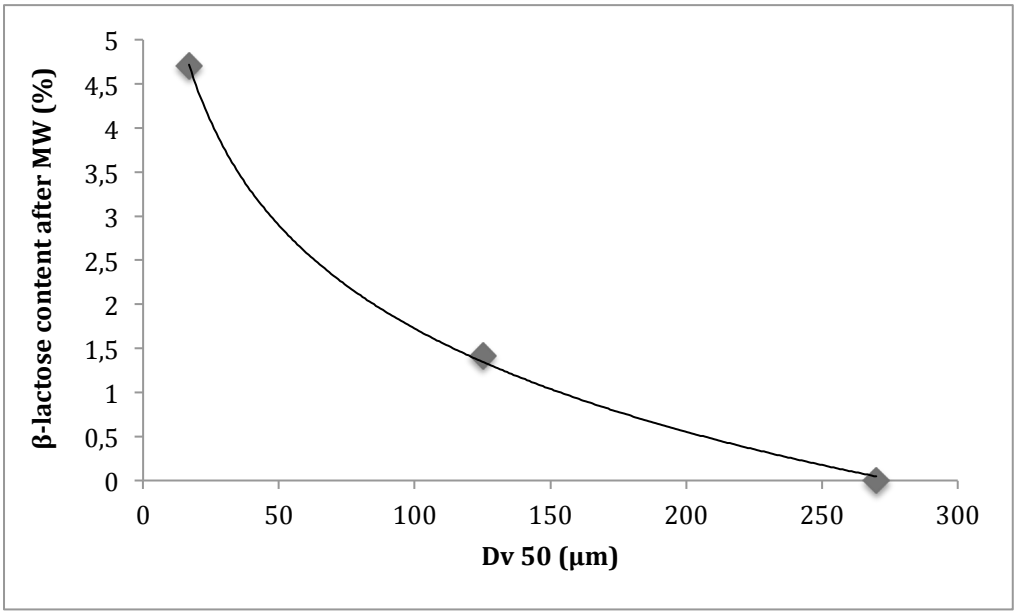

Figure 24 β-lactose formed upon microwave treatment as function of median diameter of the lactose raw material.

This result is not surprising, since the amount of β-lactose formed during the slurry production, stems for the dissolution of the external part of the raw material upon addiction of the binding solution. Therefore, the phenomenon is more pronounced for samples with high surface area (lower particle size), which were more prone to partial dissolution during the slurry production.

4.4 Procedure #4: Microwave preparation of Lactose granules + "fine" lactose using an almost saturated lactose solution as binder

It is well known that the addition of fine fraction of excipient to a coarse carrier material exerts a positive effect on the aerodynamic performance of a carrier-based inhalation mixture (X. M. Zeng et al., 1998)(Kinnunen et al., 2015). The FPF of the drug increases with the increment of fine particles concentration until

to a specific threshold value of fine content; after this point the fine concentration increment lead to a plateau or even to a decrease of the FPF.

In the present work the role of the fine particles added as material capable to alterate the morphology and the porosity of the granules during their production was investigated.

Moreover, it was decided to proceed the research work with Lactohale LH100 considering the in *vitro* results shown in the chapter 4.3.2.1

4.4.1 Size and morphological analysis of granule pores

Morphological analysis was performed in order to evaluate the porosity of the material, i.e. the size of the holes that were created among the lactose particles in the production process. The integrity of the granules was checked as well.

It has been reported that one of the factors that dominates the drug-carrier adhesion is the presence of “holes” and cavity on the lactose surface. In particular, “active sites” may be considered as areas on the lactose surface that have a high adhesion potential; drug particles adhered to these areas will subsequently be more difficult removed during the aerosolization step. Furthermore, the adhesion force increases in the presence of an irregular carrier surface presence of pits and clefts or due to larger surface area, which increases the points of contact with the drug particles.

The pore size of the produced granules was measured from the SEM pictures using the image processing and analysis program IMAGE-J® (NIH, USA). The

measurement was conducted on 50 pores of the LH 425µm granules (Figure 25); an average value of pore diameter of 181 µm was obtained.

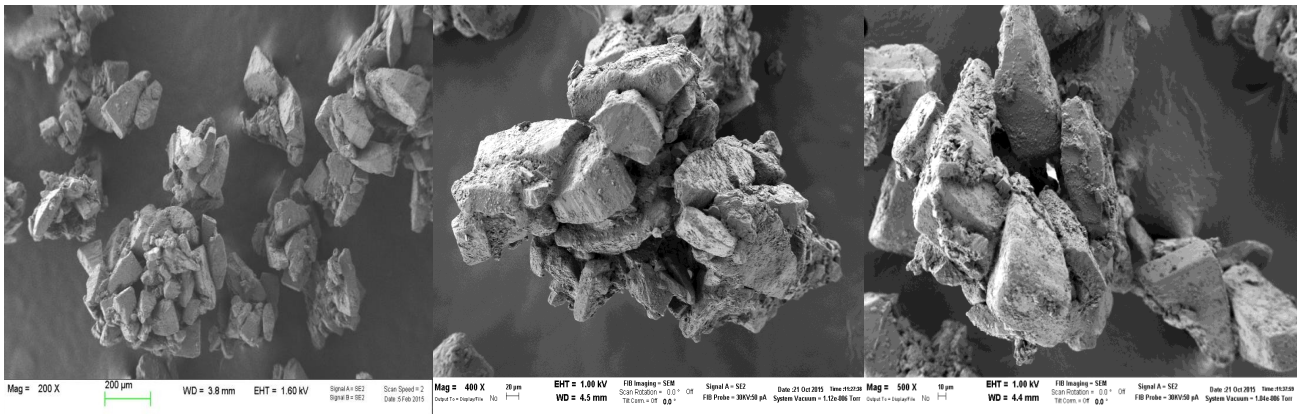

Figure 25 SEM pictures of Lactohale LH100 425 µm granules

With the aim of "filling" at least in part these cavities, the method of granules production was modified by adding different amount of "fine" lactose in different size during the slurry production.

Three ranges of "fine" carriers produced starting from Lactohale LH100 were selected:

- < 45 µm;
- < 65 µm;
- < 125 µm.

Morphological analysis on granules prepared with the "fine" <45 µm was performed. As it can be appreciated in the Figure 26 the particles of "fine" lactose were located on the lactose granules surface but it was unclear if the "fine" particles were capable to fill completely the holes. However, several "fine" particles were adhered to the cracks of surface of the coarse lactose particle and at least a partial reduction of the granules porosity was obtained.

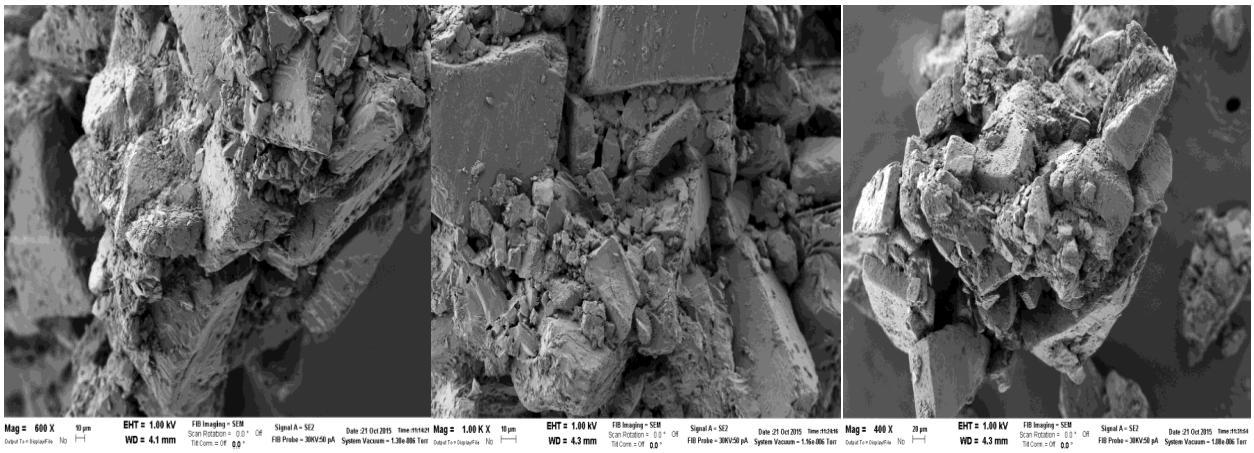

Figure 26 SEM pictures of Lactohale LH100 425 µm granules + 10 % of <45 µm fine.

4.4.2 Carriers preparation and BDP blends uniformity

The granules (425 µm) were prepared as previously described by adding the "fine" lactose in different amount during the slurry preparation or after the microwave dried. Furthermore, two other fine namely, Lactohale LH300 and Preblend Chiesi were used in the granules preparation for comparative purpose.

Table 9 shows the dose and the homogeneity of the BDP blends prepared with these granules. The blends from #1 to #14 were prepared by adding the fine portion of lactose during the slurry preparation while the blends from #15 to #17 were prepared by adding fine after the microwave drying process and #18 blend was prepared by adding "fine" <45 µm to the Lactohale LH100 425 µm granules.

As far as the granules containing different percentages of fine are concerned, the drug content was quite variable and the relative standard deviation was, in most cases, higher than 5%, which represents the acceptance limit of the EMA guideline. This high variability was related neither to the type of granule considered (% of fine) nor to the method of preparation (fine before or after the

drying process). This discrepancy could be attributed to the fact that in the mixture several aggregates of the drug were present during the preparation. The crushing of these agglomerates through the sieve, besides the loss of the active ingredient, did not guarantee a uniform distribution of the fragments in the mixture. Probably the shear stress of the Turbula® mixer was not sufficient to overcome the forces of cohesion between the particles of BDP. In fact, the shear stress in this mixer was essentially determined by the fast relapse of the coarser carrier particles during the overturning of the container.

It is possible to conclude that the mixing process has to be improved in order to reach a satisfactory drug distribution. The sieving of the API before the process and the gradual addition of the lactose carrier may represent a suitable approach.

Table 9 Drug content and uniformity of BDP/blends prepared with lactose + fine in different percentage and after the resulted granules (425 µm) were dried in the microwave (#1 to #14) and lactose granules dried in the microwave + fine in different percentage (#15 to #18). The theoretical BDP content was 100 µg/10mg.

Blend	Fine size	Materials	API µm/10 mg blend	RSD %
#1	<45 µm	BDP/LH100 + LH100 fine (5%)	96.4 ± 12.1	12.57
#2		BDP/LH100 + LH100 fine (10%)	93.6 ± 7.2	7.72
#3		BDP/LH100 + LH100 fine (30%)	82.7 ± 23.5	28.45
#4		BDP/LH100 + LH100 fine (50%)	72 ± 13.8	19.14
#5	<65 µm	BDP/LH100 + LH100 fine (5%)	98.0 ± 22.6	23.01
#6		BDP/LH100 + LH100 fine (10%)	84.5 ± 12.8	15.14
#7		BDP/LH100 + LH100 fine (30%)	100.7± 4.0	3.98
#8		BDP/LH100 + LH100 fine (50%)	114.7 ±3.2	2.72
#9	<125 µm	BDP/LH100 + LH100 fine (5%)	89.0 ± 16.7	18.74
#10		BDP/LH100 + LH100 fine (10%)	78.7 ± 11.3	14.35
#11		BDP/LH100 + LH100 fine (30%)	84.2 ± 9.0	10.75
#12		BDP/LH100 + LH100 fine (50%)	96.4 ± 16.4	17.02
#13		BDP/ LH100 + LH300 (10%)	95.1 ± 9.3	9.82
#14		BDP/ LH100 + Preblend (10%)	107.6 ± 21.6	20.07
#15		BDP/ LH100 granules + LH300 (10%)	96.8 ± 4.4	4.58
#16		BDP/ LH100 granules + preblend CHIESI (10%)	98.7 ± 4.2	4.20
#17		BDP/ LH100 raw material + preblend CHIESI (10%)	79.7 ± 2.4	3.05
#18	<45 µm	BDP/ LH100 granules + LH fine (10%)	89.7 ± 5.9	6.60

4.4.3 Aerosolization summary of BDP blends

The aerosolization performances of blends were assessed by performing *in vitro* test with the FSI. The emitted dose increase for all batch compared to the raw material (data not shown).

Figure 27 summarizes the FPF of all blends.

It is worthy underlying first of all that, the obtained FPF did not reflect the uneven drug distribution. In fact, the relative standard deviation (%) of the FPF for all formulations was within 6.93 %.

Addition of “fine” < 45 µm lactose to powder formulations has been shown to improve the dispersion and disaggregation of beclomethasone dipropionate, resulting in higher FPF compared to the blend made with the raw material and indicated the same drug detachment when the percentage of < 45 µm fine was added until 30 % compared to the lactose granules without fines.

For blend prepared with “fine” lactose < 65 µm and < 125µm, at all tested “fine” concentration, a significantly improved aerolization performance compared to LH100 raw material blend was observed while, in the range of concentrations investigated, the addition of “fine” < 65 µm and < 125 µm did not increase performance compared to granules of LH100.

These findings were in agreement with previous studies by Zeng et al. (1999), which attributed the observation to the "active site theory " with larger lactose fine being less effective in occupying the high energy binding sites on the surface of the large lactose.

The addition of fine lactose LH300 improved the drug detachment compared to the raw material but not compared to the LH100 granules. The addition of the Preblend Chiesi, afforded worse FPF compared to both reference material. This not surprising because the Preblend Chiesi contains 2% magnesium stearate which remained entrapped in the lactose granules during the slurry preparation thus losing its lubricant property on the surface of the coarse particles.

The carriers prepared by adding the fine after the microwave procedure showed different drug detachment. Blends prepared with 10% fine LH300 confirmed that the addition of fine particles improves the drug detachment compared to the blend prepared with LH100 raw material, although the performance was not higher than that obtained with the reference granules prepared without fines.

The addition of Preblend Chiesi both to raw material and to the granules after the microwave procedure almost doubled the FPF compared to the reference granules prepared without fine; this is not surprising, since the presence of magnesium stearate that could spread on the surface of both the lactose particles or granules could exert a positive effect by reducing the work of adhesion between the drug and lactose as a consequence of the coating of the carrier surface and of the lubricant effect (Tay, et al., 2010; Singh et al., 2014).

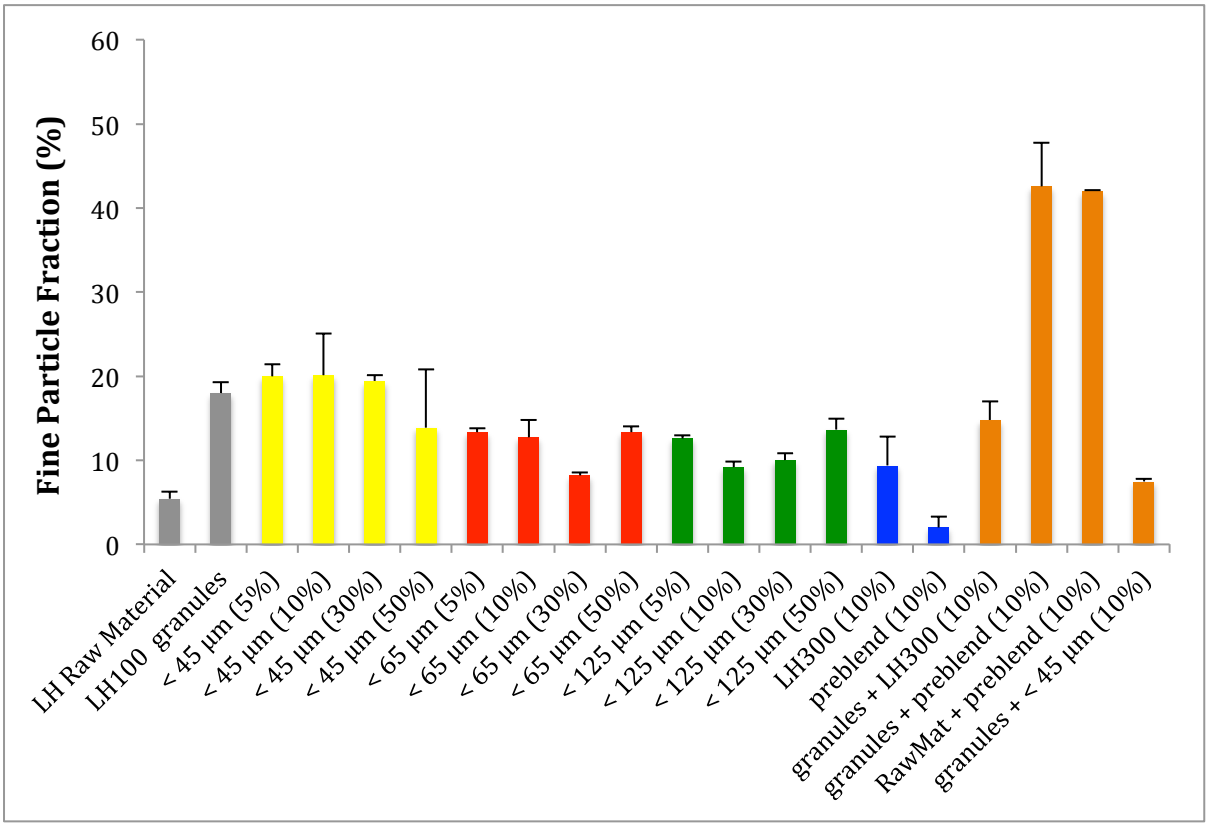

Figure 27 Fine Particle Fraction (FPF) of BDP/blends prepared with lactose + fine in different percentage and after the resulted granules (425 µm) were dried in the microwave and lactose granules (425 µm) dried in the microwave + fine in different percentage. In grey the reference material, in yellow lactose + fine <45 µm, in red lactose + fine < 65 µm, in green lactose + fine < 125 µm, in blue lactose + fine commercial products and in orange lactose + fine added after the microwave drying process.

4.4.4 Powder dry dispersion

A set of physical measurement were performed in order to get more insight into the physical characteristics of the prepared granules aiming at collecting information relevant to the practical usability of such carriers and on the aspects related to the interaction between the drug and the prepared carriers.

First of all, the dry dispersility was carried out by using the Quicpic/Rodos apparatus. The analysis was conducted on LH100 425 µm granules, LH100 425 µm granules + 10 % of 45 µm "fine", LH100 425 µm granules + 30 % of 45 µm

"fine" and LH100 425 µm granules + 10 % of 125 µm "fine". For all samples the "fine" portion was added during the slurry preparation.

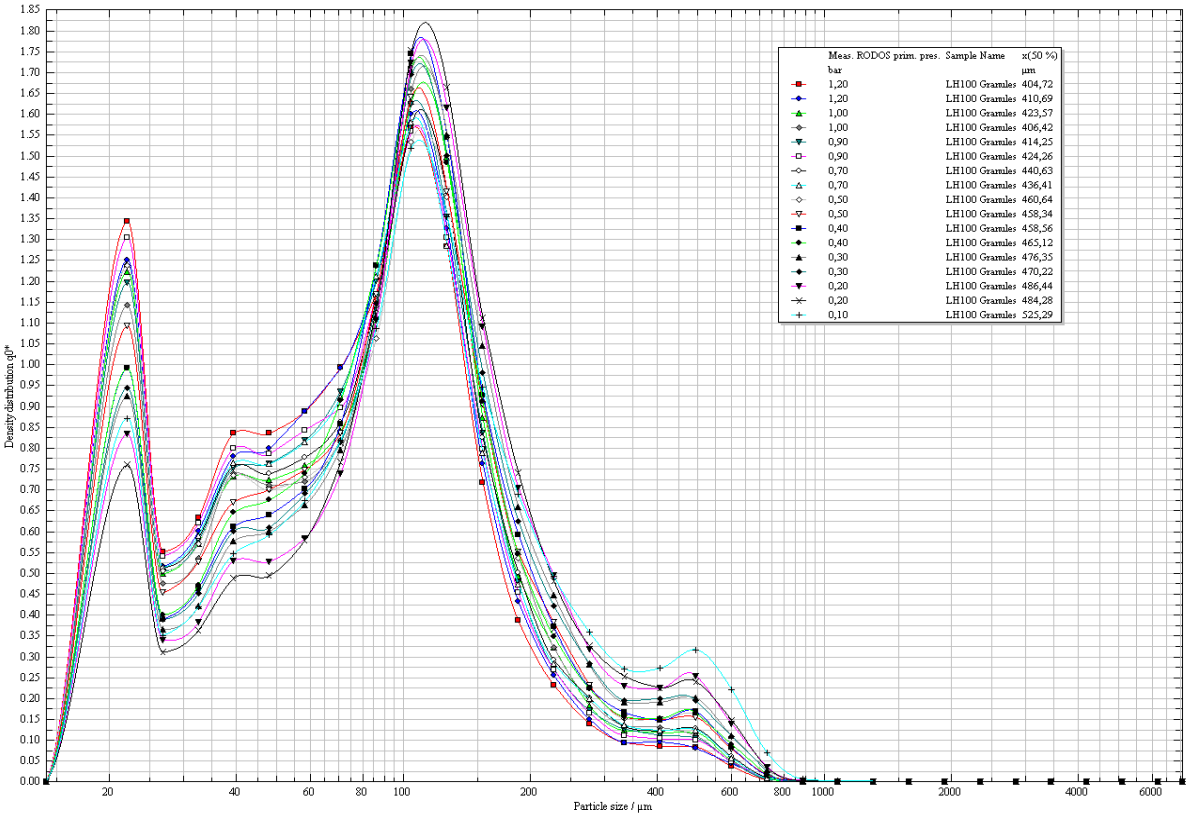

Figure 28 Qicpic dry dispersion of LH100 425 µm granules as a number distribution that indicates the percentage of the particles according to the particle size as a function of the total number of the particles.

The aim of this measurement was to evaluate the hardness of the granules at different pressure in order to determinate a specific breaking point; Figure 28 shows the dry dispersion of LH100 425 µm granules as number distribution (QO) that indicates the percentage of the particles according to the particle size as a function of the total number of the particles.

As it can be appreciated from the data reported in the Figure 28, the particle size of the granules decreased constantly by increasing the applied pressure and no breaking point was identified. The same behaviour was observed for all the

prepared granules (data not shown). It is also possible to note the rapid granules disaggregation even at 0.1 bar.

Therefore, the Q0 distribution of the granules was evaluated by taking in account a cut off of 150 µm.

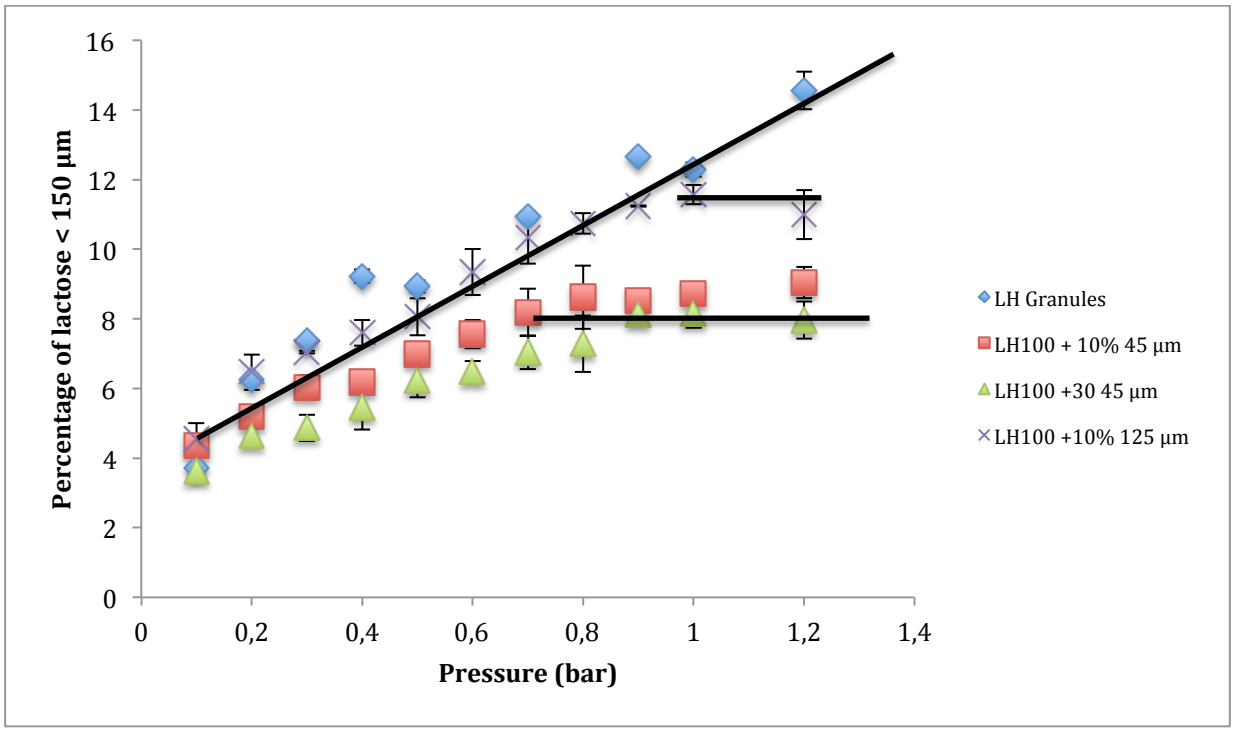

Figure 29 Qicpic dry dispersion of lactose granule samples considering the percentage of fine < 125 µm as a function of the applied pressure.

Figure 29 shows the percentage of lactose with a particle size lower than 150 µm generated by applying a pressure from 0.1 to 1.2 bar. It can be observed that the addition of "fine" increased the hardness of the granules and the cohesion between the lactose particles. This effect was more pronounced when the added "fine" was smaller and in higher amount. In fact, the carriers with 45 µm "fine" reached a plateau around 0.7-0.8 bar: the increase of pressure did not increase the percentage of the particle with a particle size lower then 150 µm. The

percentage of particles having size < 150μm corresponding to said plateau was higher for the granules containing "fine" at 125 μm compared to that of the granules prepared with the "fine" at 45μm. In this latter case the increase of the content of "fine" further reduced the percentage of particles having size < 150 μm at the plateau. This behaviour could explained by considering that the presence of "fine" created bridges between the larger particles making stronger the granules. The increment of cohesion among the lactose particles should improve the fluidization and aerosolization behaviour and lead to higher aerodynamic dispersion forces within inhalation device (Shur et al. 2008).

4.4.5 Specific Surface Area

The specific surface area (SSA) was evaluated in order to understand if the addition of "fine" could fill the spaces present in the lactose granules.

Figure 30 depicts two opposite theoretical situations that could occur when the fine is added to the course particles; on the left-hand side it is described the situation in which the fine particles fill completely the entire carrier surface leading to a decrease of the specific surface area whereas on the right-hand side a situation where the fine particles fill only partially the carrier surface is depicted; in this latter case, if we consider the lactose fine as a spherical particles, the surface of the carrier covered is complementary to the sphere, hence the specific surface area remain almost unchanged.

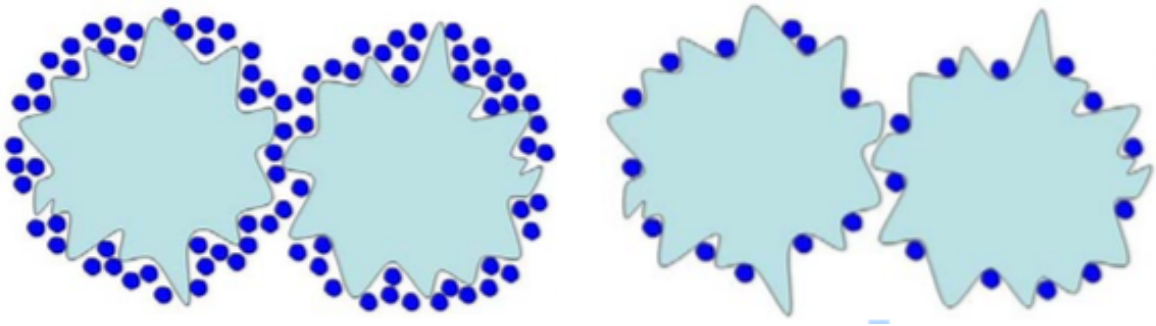

Figure 30 Theroretical configurations of lactose course particle (in green) + fine particles (in blue).

The specific surface (SSA) area analysis was conducted on LH100 425 µm granules, LH100 425 µm granules + 10 % of 45 µm "fine", LH100 425 µm granules + 30 % of 45 µm "fine", LH100 425 µm granules + 10 % of 125 µm "fine" and on the < 45 µm fine particles. Also in this case the "fine" portion was added during the slurry preparation.

Table 10 reports the results of BET analysis conducted on the four lactose granules treated with microwave as well as on the 45 µm "fine" particles.

The SSA of the LH100 granules was similar to that of LH100 425 µm granules prepared with 10% of 125 µm "fine". This can be ascribed to the fact that the "fine" added to the carrier presented the same dv50 of the raw material while it is not surprising that the increase of the percentage of "fine" increased the specific surface area of the carrier.

Table 10 Specific surface area of the LH100 granules and LH100 granules prepared with different amount of "fine" of different size.

	LH100 (m^2/g)	**LH100 + 10% < 45µm (m^2/g)**	**LH100 + 30% < 45µm (m^2/g)**	**LH100 + 10% <125µm(m^2/g)**	**fine <45 µm (m^2/g)**
	0.1542	0.213	0.2915	0.1509	0.6222
	0.1417	0.2285	0.3446	0.1664	0.6475
	0.1643	0.2182	0.3102	0.149	0.6796
Mean	**0.1534**	**0.2199**	**0.3154**	**0.1554**	**0.6498**
S. D.	0.0113	0.0079	0.0269	0.0095	0.0288

To assess a correlation between the BET data and to understand if the SSA increment observed was directly proportional to the percentage of "fine" added, the theoretical surface area for the carriers with "fine" was calculated as the weighted mean of the experimental surface areas of carrier without "fine" and the experimental SSA of "fine" added at 10% or 30% w/w (Table 11). The good agreement between measured and calculated data indicated that the SSA increment observed for the granules was completely ascribed to the contribution of "fine" particles added to the lactose granules.

Table 11 Theoretical and experimental surface area of carrier + "fine".

	LH100 + 10% <45 µm (m^2/g)	LH100 + 30% <45 µm (m^2/g)
Experimental SSA	0.22± 0.008	0.31 ± 0.03
Theoretical SSA	0.20	0.33

4.4.6 Powder Flowability

The rheological properties of the prepared granules were investigated with the FT4 apparatus. The flowability of Lactohale LH100 raw material was determined for comparative purpose.

Table 16 reports the Basic Flowability Energy (mJ) and the Specific Energy (mJ) of the powder samples. Interestingly a marked difference between the raw material and treated material can be observed. The BFE of the treated samples were significantly lower than that of the raw material indicating better flow property compared to the raw material. The reason of this behaviour can be easily attributed to the particle higher size of the carrier, considering that particles with a low particle size are more cohesive and thus require more energy to flow. The best result was obtained with the carrier LH100 425 μm granules + 30% of "fine" with a BFE value three times lower than that of the raw material. This data are in agreement and confirm the data relevant to the granule strength determined with the dispersibility test (see 4.4.4): here the carrier remained intact after the stress imposed by the blade of the powder rheometer indicating that it was not subjected to the segregation phenomenon that has a negative effect on the BFE.

The specific energy is mostly related to the particle cohesion, so in general a SE lower then 5 indicates low particle cohesion, a SE between 5 and 10 indicates a moderate cohesion and SE higher than 10 indicates a an higher particle

cohesion. The obtained SE values are reported in Table 12. It can be appreciated that all granules showed a SE lower than 5 while the value relevant to the raw material was slightly higher than 5. This data indicate a lower particle cohesion of the treated materials also in this case ascribable to the particle size of this carriers and further confirm the BFE results previously described.

Table 12 BFE and SE of LH100 raw material, LH100 granules obtained with microwave. Mean values and standard deviation.

	BFE (mJ)	**SE (mJ/g)**
LH100 raw material	455 ± 31.8	5.3 ± 0.1
LH100 Granules	188 ± 33.8	3.2 ± 0.9
LH100 +10% "fine" 45 µm	286 ± 9.9	4.7 ± 0.1
LH100 +30 % "fine" 45 µm	148 ± 28.0	3.1 ± 0.1
LH100 +10% "fine" 125 µm	278 ± 67.5	3.8 ± 0.4

4.4.7 Contact angle, Surface Energy and Work of Adhesion and Cohesion

Contact angle (Θ) measurements were conducted on LH100 425 µm granules, LH100 425 µm granules + 10% of 45 µm "fine", SS and BDP by using two polar liquids, water and ethylene glycol, and a non-polar liquid, di-iodomethane. The obtained values of contact angles are summarized in the Table 13. Contact angle indicates the degree of wetting when a solid and liquid interact. The lower the contact angle the greater the wettability.

The obtained results indicate that, as expected, the BDP particles presented a more non-polar surface as opposed to SS and lactose granules; furthermore the BDP/water contact angle showed a value higher then 90° that indicates the BDP hydrophobic nature.

Table 13 Contact angle of lactose granules and model drugs with three different liquids. Mean values and standard deviation

	Θdi-iodomethane (°)	ΘEthylene glycol (°)	Θwater (°)
LH100 425 µm granules	60.11 ± 0.71	63.30 ± 3.89	74.44 ± 0.70
LH100+ 10% <45 µm fine 425 µm granules	59.45 ± 0.09	63.63 ± 5.58	71.48 ± 0.98
SS	60.77 ± 2.37	75.34 ± 5.72	85.11 ± 3.13
BDP	35.90 ± 1.00	31.2 ± 4.25	92.1 ± 0.93

The values of contact angle were used to compute the surface free energy according to equation 3.

Table 14 shows the results of surface free energy where the γ^{LW} indicates the dispersive part and γ^{AB} indicates the polar part. The obtained results are not surprising since the lactose samples had similar total energy to SS while the value relevant to BDP reflected its non-polar nature with a predominant dispersive energy value.

Table 14 Values of surface free energy (mN/m) calculated using the Good and van Oss equation.

	γ^{TOT} *a*)	γ^{LW}	γ^{AB} *b*)	γ^{+}	γ^{-}
LH100 425 µm granules	30,87 ± 0.99	28,64 ± 0.34	2,23 ± 0.91	21,50 ± 7.86	0,07 ± 0.05
LH100 + 10% 45 µm 425 µm granules	31,62 ± 1.62	29,02 ± 0.04	2,60 ± 1.62	22,44 ± 7.28	0,11 ± 0.09
SS	32,39 ± 2.85	28,25 ± 1.14	4,14 ± 2.47	14,32 ± 7.30	0,35 ± 0.27
BDP	43,87 ± 1.15	41,79 ± 0.39	2,08 ± 1.03	16,67 ± 7.14	2,04 ± 1.41

a) $\gamma^{TOT} = \gamma^{LW} + \gamma^{AB}$
b) $\gamma^{AB} = 2\sqrt{\gamma^{+}\gamma^{-}}$

Finally, when comparing the work of cohesion of the drugs with the work of adhesion (Table 15) with each carrier, it was observed that the work of cohesion was much higher than the work of adhesion with all lactose granules in the case of BDP, while the two figures were comparable in the case of SS. This indicates that when BDP is mixed with this lactose carrier the particles of BDP have a more pronounced tendency to adhere to each other than to the lactose carriers. Furthermore, the work of adhesion of BDP with the granules was higher compared to the work of adhesion of SS. This allows explaining the difference observed in the aerosolization performance of the two drugs as SS/lactose blends requires less energy to be separated compared to BDP/lactose blends.

Table 15 Work of cohesion and of adhesion (mN/m) of lactose samples and model drugs.

Work of cohesion				Work of adhesion		
					SS	BDP
LH100 425 µm granules	LH100 425 µm granules +10% 45 µm	SS	BDP	LH100 425 µm granules	63.8	74.8
				LH100 425 µm granules +10% 45 µm	64.5	75.8
61.7	63.2	64.8	87.7			

4.5 High drug dose blends

High drug dose DPIs formulations are traditionally manufactured for the delivery of antibiotic such as tobramycin (TOBI Podhaler, Novartis), colistimethate sodium (Colobreath, Forest Laboratoris) or mannitol used as a drug for the treatment of cystic fibrosis (Bronchitol).

High dose delivery is a challenging issue in the performance of carrier based DPIs formulation due to the inefficient drug/carrier separation.

This part of the project was focused on the investigation of the performance of blends produced with high drug content. In particular, BDP was employed as model drug and lactose granules were compared to reference lactose, Capsulac.

4.5.1 High drug dose blends homogeneity

The blends were produced by mixing 10 % w/w of BDP with different types of LH100 425 µm granules, and Capsulac. The BDP content in the prepared blends (Table 16) ranged between 81% and 100% with a relative standard deviation

always lower than 5%, except for the blend prepared whit the granules and 10 % of magnesium stearate (after MW drying).

This satisfactory homogeneity was the results of the pre-sieving of BDP with half part of the carrier that reduced significantly the formation of drug agglomerates during the Turbula mixing.

Table 16 Drug content and uniformity of high drug dose blends prepared with granules and Caspulac containing different "fines".

Type of formulation	BDP mg/10 mg of blend	RSD%
Fines added during slurry preparation		
425 µm granules + 10% fine <45µm	0.91 ± 0.02	1.89
425 µm granules + 10% fine MgSt	0.90 ± 0.04	4.33
Fines added after microwave drying		
425 µm granules + 10% fine <45µm	0.89 ± 0.02	2.63
425 µm granules + 10% Preblend	1.00 ± 0.02	1.86
425 µm granules + 10% MgSt	0.95 ± 0.05	5.39
Capsulac + 10% fine <45µm	0.81 ± 0.03	3.18
Capsulac + 10% Preblend	0.84 ± 0.03	3.31
Capsulac + 10% MgSt	0.93 ± 0.03	3.24

4.5.2 Aerodynamic assessment of high drug dose blends

The in vitro aerosolization was performed also in this case with the FSI apparatus. Table 17 highlights the emitted dose of the blends; lactose granules showed the best performance when the lubricant, MgSt, was added to the granules after the microwave drying process. Nevertheless, all the ED were not significant different among the studied blends.

Table 17 Emitted dose of high drug dose blends. **Pre MW= fine added during the slurry preparation; Post MW= fine added after the microwave drying. Mean values and standard deviation.**

	425 µm granules + 10% fine <45 µm (PRE-MW)	**425 µm granules** + 10% fine MgSt (PRE-MW)	**425 µm granules** + 10% fine <45µm (POST-MW)	**425 µm granules** + 10% Preblend (POST-MW)	**425 µm granules** + 10% fine MgSt (POST-MW)	**Capsulac** + 10% fine <45µm (POST-MW)	**Capsulac** + 10% Preblend (POST-MW)	**Capsulac** + 10% fine MgSt (POST-MW)
Emitted Dose (µg)	609.1 ± 75.1	567.6 ± 20.6	668.3 ± 19.4	694.5 ± 3.0	757.1 ± 23.6	576.2 ± 9.1	586.1 ± 45.0	633.6 ± 33.0

The FPF of these blends are reported in Figure 31; in green are represented the blend prepared by adding the fine material to the lactose raw material during the slurry preparation, in red the blend prepared by adding the fine materials to the granules after the microwave drying process and in blue the blend prepared by adding the fine material to the Capsulac.

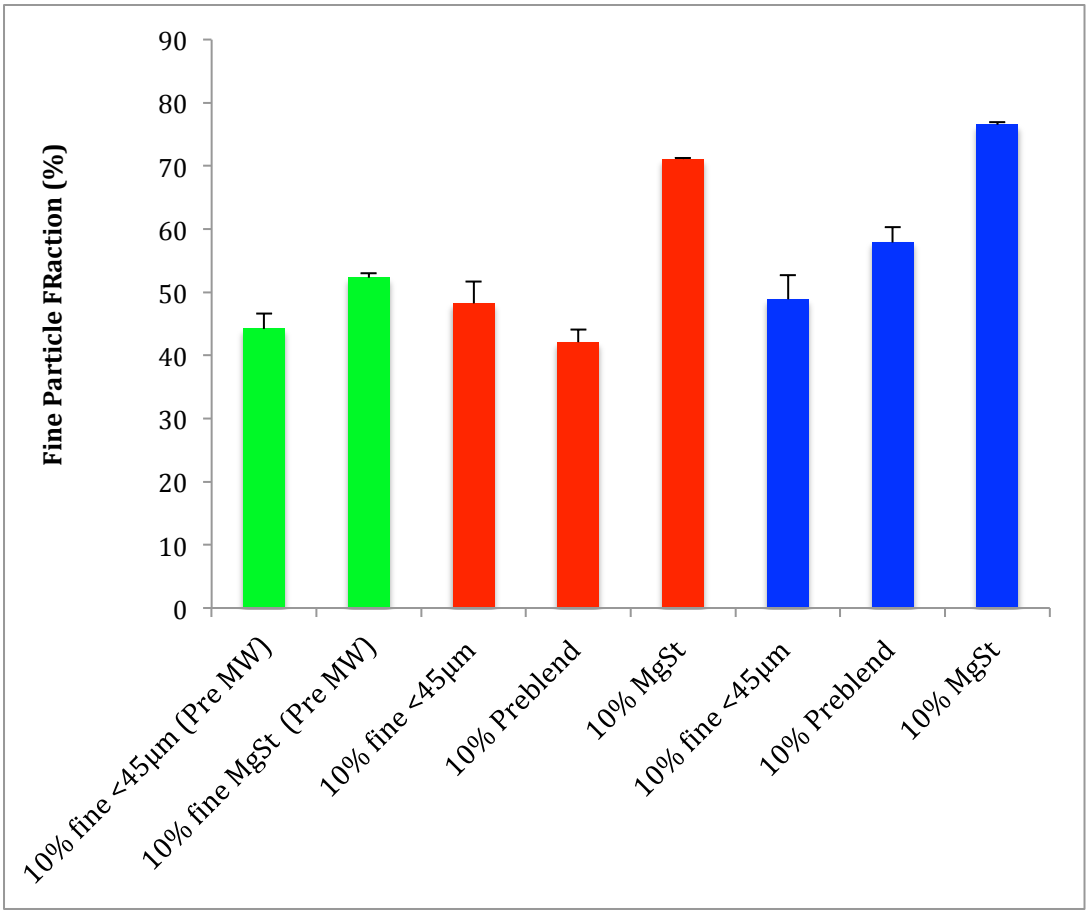

Figure 31 FPF of high BDP dose blends. The bars represent the standard deviation.

As it was expected, magnesium stearate raised the FPF up to 71.1 % and 76.5 % of LH100 425 µm granules and Capsulac respectively, when it was added after the microwave drying process, i.e. directly to the granules. In addition contrary to what was previously presented, here the addition of magnesium stearate during the slurry preparation resulted in an increase the drug detachment up to 52.3 %, likely due to the fact that part of the high amount of magnesium stearate (10%) added to the lactose did not remain entrapped in the granules and positioned at the granules surface where it exerted its lubricant action.

Finally, LH100 425 µm granules + 10% of "fine" lactose showed a higher FPF compared to LH100 425 µm granules + preblend indicating that the magnesium

stearate present in the Preblend did not affect the BDP detachment and that the addition of 10 % of "fine" to the granules reduced the interaction of the drug with coarse lactose particles making more easy the drug aerosolization.

4.6 Procedure #4: Vacuum oven preparation of lactose granules using an almost saturated lactose solution

The investigated microwave drying method have proved to be a suitable process to produce lactose granules, to be used as suitable carrier for the preparation mixtures with drugs

An alternative method adopting the same approach but carried out with more "traditional" instruments such as a vacuum oven instead of a microwave drier was investigated with the aim of assessing whether granules with properties comparable to those of the granules prepared with microwave drying could be prepared.

Lactohale LH100 was chosen as election material due to the promising results obtained with the *procedure #2.* Moreover, the mixing time (1 min and 10 min) to produce slurry and the slurry granulation size (425 μm and 600 μm) were investigated.

4.6.1 Solid state characterization

4.6.1.1 Differential Scanning calorimetry

Figure 32 shows the comparison of the DSC traces of Lactohale LH100 raw material, LH100 425 µm granules prepared with vacuum oven and LH100 425 µm granules prepared by microwave drying. The thermal behaviour of the granueles prepared by vacuum oven was superimposable to that of the granules obtained by microwave drying. In particular, both traces did not present the exothermic peak around 180°C which was instead observed with the starting raw material.

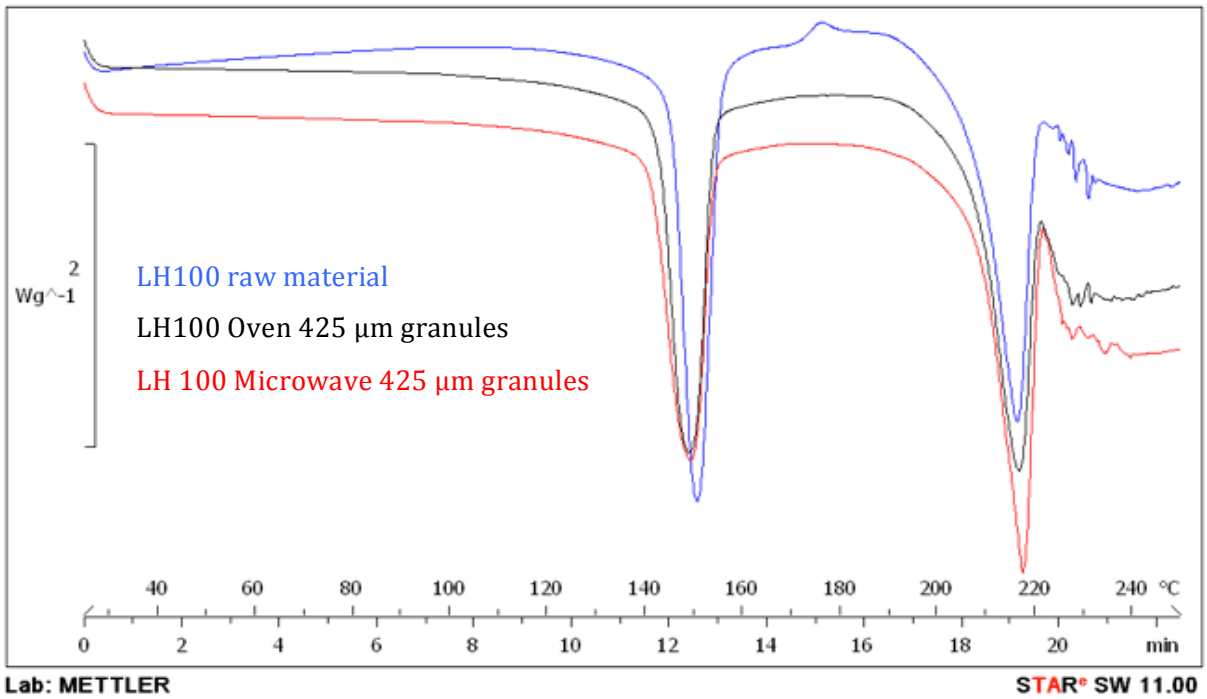

Figure 32 in blue DSC trace of lactose LH100 raw material, in black DSC trace of lactose 425 µm granules dried in the oven, in red DSC trace of lactose 425 µm granules dried in the microwave.

4.6.1.2 X-Ray powder Diffraction (XRPD)

Figure 33 shows in green and in blue the diffraction patterns of the samples dried with the vacuum oven and the microwave respectively in comparison with

the starting material diffraction pattern (in red); the diffractograms were very similar to each other and exhibited the characteristic pattern of α-lactose monohydrate (Gombás et al., 2003).

Since the distinctive peaks of each polymorph of lactose lie almost in the same regions of the diffraction pattern, it was not possible to evaluate the presence of polymorphs different from the α-monohydrate while it is important to underline how both the dry processes did not induce changes in the samples crystallinity.

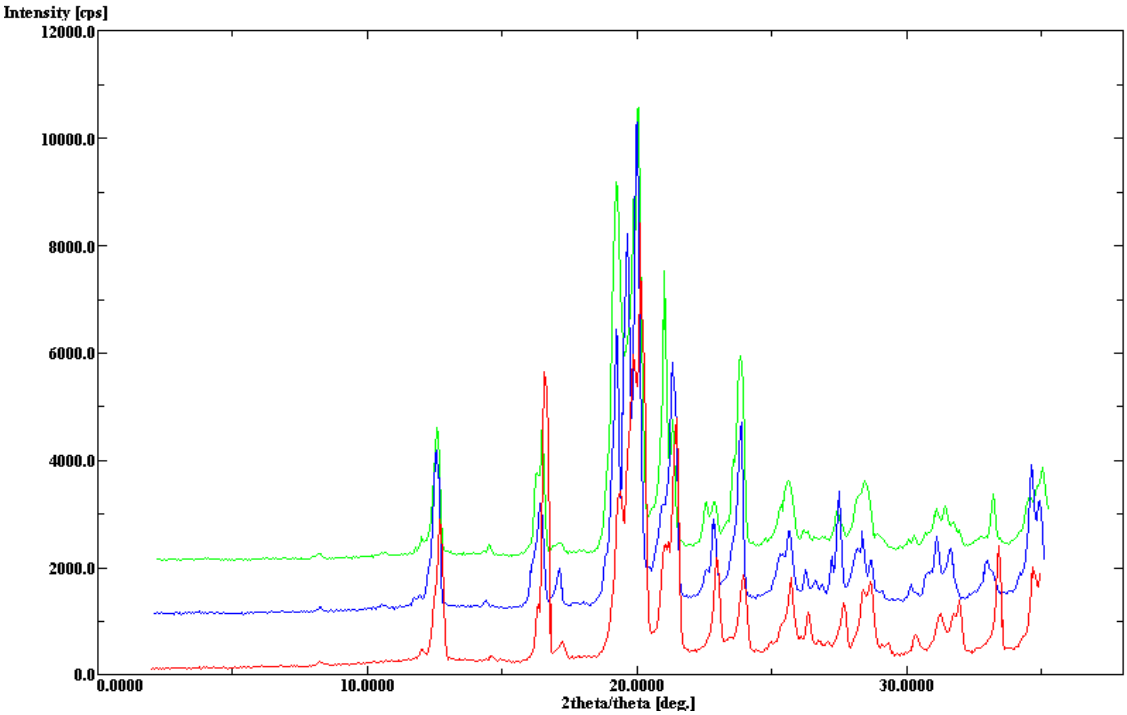

Figure 33 XRPD patterns of lactose, in green lactose LH100 425 µm granules dried in the oven, in blue lactose LH100 425 µm granules dried in the microwave, in red DSC trace of lactose LH100 raw material.

4.6.1.3 Fiability test

The friability test afforded a very low value (0.4%) indicating that the process of drying in the vacuum oven did not make the granules brittle.

4.6.2 Carrier preparation

Different samples were prepared as described in section 3.2.1.3 and they are listed below:

#1. LH100 mixing time to produce the slurry = **1 min;** sieving at **425 µm;** drying in **microwave**;

#2. LH100 mixing time to produce the slurry = **10 min** sieved at **600 µm;** drying in **microwave**;

#3. LH100 mixing time to produce the slurry = **1 min** sieved at **425 µm;** drying in **oven**;

#4. LH100 mixing time to produce the slurry = **10 min** sieving at **600 µm;** drying in **oven**;

#5. LH100 mixing time to produce the slurry = **10 min** sieving at **425 µm;** drying in **microwave**;

#6. LH100 mixing time to produce the slurry = **1 min** sieving at **600 µm;** drying in **microwave**;

#7. LH100 mixing time to produce the slurry = **10 min** sieving at **425 µm;** drying in **oven**;

#8. LH100 mixing time to produce the slurry = **1 min;** sieving at **600 µm;** drying in **oven**.

4.6.3 BDP/lactose blends content uniformity

BDP and lactose were mixed in a ratio 1:100 (w/w) to obtain a binary mixture. BDP was successfully blended with carrier produced with both methods; as show the Table 18 the relative standard deviation was less then 5% for all the prepared blends.

Table 18 Drug content and uniformity of BDP blends prepared with lactose dried with the oven or microwave.

	API µm/10 mg blend	RSD %
1 min 425 µm microwave	99.4 ± 1.80	1.81
1 min 600 µm microwave	98.1 ± 1.33	1.36
1 min 425 µm oven	99.3 ± 2.79	2.80
1 min 600 µm oven	94.3 ± 3.94	4.11
10 min 425 µm microwave	93.3 ± 4.52	4.84
10 min 600 µm microwave	94.8 ± 4.53	4.77
10 min 425 µm oven	104.6 ± 4.03	3.84
10 min 600 µm oven	101.2 ± 3.60	3.56

4.6.4 In vitro aerosolization of BDP/lactose blends

Table 19 summarizes the aerosolization performance data of the prepared blends. The emitted doses of all blends prepared were higher or comparable to that of the blend prepared with the raw material. As far as the Fine particle dose is concerned, for the microwave blends it ranged between 7.18 µg and 12.5 µg and for the oven blends between 11.19 µg and 17.33 µg while blend prepared with the raw material afforded an FPD of 5.4 µg

The blend prepared with the granules dried in the oven presented a FPF higher than that obtained with the blend prepared with raw material, whereas it was not significantly different from that of the blend made with the microwave dried granules. Moreover, neither the slurry mixing time nor the granulation size had a significant influence on the drug detachment.

Table 19 Aerosolization performance of BDP/blends prepared with lactose dried with the oven or microwave.

	Emitted Dose (µg)	FPD (µg)	FPF (%)
Lactohale Raw material	66.9 ± 6.7	5.4 ± 1.2	5.4 ± 0.9
1 min 425 µm MW	77.41 ± 11.6	8.85 ± 1.6	10.37 ± 1.66
1 min 600 µm MW	77.86 ± 5.9	7.18 ± 4.0	7.29 ± 4.3
1 min 425 µm O	71.31 ± 3.9	13.65 ± 2.8	15.72 ± 2.5
1 min 600 µm O	67.31 ± 9.1	17.33 ± 1.8	18.36 ± 1.8
10 min 425 µm MW	66.11 ± 1.36	7.19 ± 1.1	8.50 ± 2.1
10 min 600 µm MW	59.1 ±10.2	12.5 ± 5.3	11.8 ± 3.4
10 min 425 µm O	76.06 ± 7.3	11.19 ± 0.3	12.66 ± 0.2
10 min 600 µm O	62.07 ± 6.9	12.69 ± 2.14	13.91 ± 0.7

For these reasons is possible to conclude that the vacuum oven drying method proved to be a suitable method to produce lactose granules and an alternative method to the microwave drying process for manufacturing lactose granules.

However, the microwave drying process presents a main advantage with respect to the vacuum oven drying process as it requires a very low drying time (5 minutes).

5 Conclusions

The present research project was focused on the development of an innovative method to produce lactose granules to be used as carrier for inhalation.

The method implies the formation of a slurry starting from different raw materials using water as a binder solution. The slurry was dried with microwave. After sieve test the resulted lactose samples were fragile or wet depending to the amount of water added to produce the slurry and to the microwave power set for the dry process.

A Design of Experiment put into evidence the main variables affecting the process.

Once identified the proper process conditions the method was implemented replacing water with an almost saturated solution of the same lactose as binder. The formation of the granules is therefore obtained by wet granulation by forcing the slurry to pass to a predetermined mesh size. This phase is followed by a rapid drying by microwave irradiation. The optimisation of the process led to granules, having highly resistance to mechanical stress and with better aerodynamic performance both with BDP and SS compared to the starting lactose.

Granules with similar characteristics can be produced also by drying the slurry in a vacuum oven; this represents therefore a valid, although less innovative and more time-consuming alternative to the microwave drying.

The addition of fine lactose, as third component, does not lead to results that can be generalized, since they depend on the type and on the percentage of fine lactose added as well as on the mode of fine addition (during the slurry preparation or after the granules drying).

The results so far suggest that the positive effect of the ternary component on the drug dispersion during aerosolization may be explained by the occupation of the active site, both on the coarse lactose particle surface and in the spaces within the coarse lactose particles, resulting in a easier detachment of drug particles.

On this basis a study of flowability of the carrier was evaluated. Qicpic dry dispersion test demonstrated that the addition of fine improve the granules toughness in particular the addition of “fine” lactose during the slurry preparation led to the formation of granules more compact that submitted to elevate pressure maintained its particle size distribution.

LH100 425 μm granules with and without fine proved to be more flowable and less cohesive compared to the raw material and reference material (Capsulac) as evidenced by the rheometric tests.

Finally, the *in vitro* aerosolization of the high drug dose blends demonstrated the usability of these granules also for the preparation of drug-carrier mixture with drug payload significantly higher than that typically adopted for bronchodilators and anti-inflammatory drugs.

As a general conclusion, an innovative and easy scalable method to produce a "customized" lactose carrier was developed. The satisfactory results obtained by the *in vitro* aerosolization and the good characteristics of flowability and mechanical resistance allows to foresee a promising further development of the these granules in particular for the manufacture of multidose DPI that require not only a good drug detachment but also an excellent flowability to assure consistent drug aerosolization after several administration.

6 References

Begat, P., Morton, D. A. V, Staniforth, J. N., & Price, R. (2004). The cohesive-adhesive balances in dry powder inhaler formulations I: Direct quantification by atomic force microscopy. *Pharmaceutical Research, 21(9), 1591-1597. http://doi.org/10.1023/B:PHAM.0000041*

Biresaw G., & Carriere C. J. (2001). Correlation between mechanical adhesion and interfacial properties of starch/biodegradable polyester blends. *Journal of Polymer Science, Part B: Polymer Physics*, *39*(9), 920–930. http://doi.org/10.1002/polb.1067

Buttini F., Brambilla G., Copelli D., Sisti V., Balducci A. G., Bettini R., & Pasquali I. (2016). Effect of Flow Rate on In Vitro Aerodynamic Performance of NEXThaler ® in Comparison with Diskus ® and Turbohaler ® Dry Powder Inhalers. *Journal of Aerosol Medicine and Pulmonary Drug Delivery*, *29*(2), 167–178. http://doi.org/10.1089/jamp.2015.1220

Chen J., Wang J., Li R., Lu A., & Li, Y. Thermal and X-ray Diffraction Analysis of Lactose Polymorph, 102Procedia Engineering 372–378 (2015). Elsevier B.V. http://doi.org/10.1016/j.proeng.2015.01.165

Chow A. H. L., Tong H. H. Y., Chattopadhyay P., & Shekunov B. Y. (2007). Particle engineering for pulmonary drug delivery. *Pharmaceutical Research*, *24*(3), 411–437. http://doi.org/10.1007/s11095-006-9174-3

Claus S., Weiler C., Schiewe J., & Friess W. (2014). How can we bring high drug doses to the lung? *European Journal of Pharmaceutics and Biopharmaceutics*, *86*(1), 1–6. http://doi.org/10.1016/j.ejpb.2013.11.005

Colombo P., Traini D., Buttini F., 2013. Inhalation Drug Delivery: Techniques and Products. John Wiley & Sons, Ltd

Crowder T. M., Louey M. D., Sethuraman V. V., Smyth H. D. C., & Hickey A. J. (2001). 2001: An odyssey in inhaler formulation and design. *Pharmaceutical Technology*, *25*(7), 99–113.

Retrieved from http://www.scopus.com/inward/record.url?eid=2-s2.0-0034918105&partnerID=tZOtx3y1

De Boer A. H., Gjaltema D., Hagedoorn P., & Frijlink H. W. (2002). Characterization of inhalation aerosols: A critical evaluation of cascade impactor analysis and laser diffraction technique. *International Journal of Pharmaceutics*, *249*(1–2), 219–231. http://doi.org/10.1016/S0378-5173(02)00526-4

De Boer A. H., Hagedoorn P., Gjaltema D., Goede J., & Frijlink H. W. (2003). Air classifier technology (ACT) in dry powder inhalation: Part 1. Introduction of a novel force distribution concept (FDC) explaining the performance of a basic air classifier on adhesive mixtures. *International Journal of Pharmaceutics*, *260*(2), 187–200. http://doi.org/10.1016/S0378-5173(03)00250-3

Della Bella A., Müller M., Soldati L., Elviri L., & Bettini R. (2016). Quantitative determination of micronization-induced changes in the solid state of lactose. *International Journal of Pharmaceutics*, *505*(1–2), 383–393. http://doi.org/10.1016/j.ijpharm.2016.04.015

Dickhoff B. H. J., De Boer A. H., Lambregts D., & Frijlink H. W. (2005). The interaction between carrier rugosity and carrier payload, and its effect on drug particle redispersion from adhesive mixtures during inhalation. *European Journal of Pharmaceutics and Biopharmaceutics*, *59*(1), 197–205. http://doi.org/10.1016/j.ejpb.2004.07.005

Döring G., Flume P., Heijerman H., & Elborn J. S. (2012). Treatment of lung infection in patients with cystic fibrosis: Current and future strategies. *Journal of Cystic Fibrosis*, *11*(6), 461–479. http://doi.org/10.1016/j.jcf.2012.10.004

Edwards D. A., Hanes J., Caponetti G., Hrkach, J., BenJebria, A., Eskew, M. Lou, … Langer, R. (1997). Large Porous Particles for Pulmonary Drug Delivery. *Science*, *276*(5320), 1868–1871. http://doi.org/10.1126/science.276.5320.1868

Emmett, P. H. (1936). Gases i n Multimolecular Layers, *407*(1). http://doi.org/citeulike-

article-id:4074706\rdoi: 10.1021/ja01269a023

Ferrari F., Cocconi D., Bettini R., Giordano F., Santi P., Tobyn M., … Colombo P. (2004). The surface roughness of lactose particles can be modulated by wet-smoothing using a high-shear mixer. *AAPS PharmSciTech*, *5*(4), e60. http://doi.org/10.1208/pt050460

Figura L. O. (1993). The physical modification of lactose and its thermoanalytical identification. *Thermochimica Acta*, *222*(2), 187–194. http://doi.org/10.1016/0040-6031(93)80551-K

Form A. (2013). European Medicines Agency -, (June), 4–6. http://doi.org/10.1016/S0140-6736(10)60785-4

Freeman R. (2007). Measuring the flow properties of consolidated, conditioned and aerated powders - A comparative study using a powder rheometer and a rotational shear cell. *Powder Technology*, *174*(1–2), 25–33. http://doi.org/10.1016/j.powtec.2006.10.016

Frijlink H. W., & de Boer A. H. (2005). Trends in the technology-driven development of new inhalation devices. *Drug Discovery Today: Technologies*, *2*(1), 47–57. http://doi.org/10.1016/j.ddtec.2005.05.020

Geller D. E., Weers J., & Heuerding S. (2011). Development of an inhaled dry-powder formulation of tobramycin using PulmoSphere™ technology. *Journal of Aerosol Medicine and Pulmonary Drug Delivery*, *24*(4), 175–82. http://doi.org/10.1089/jamp.2010.0855

Gombás Á., Antal I., Szabó-Révész P., Marton S., & Erõs I. (2003). Quantitative determination of crystallinity of alpha-lactose monohydrate by Near Infrared Spectroscopy (NIRS). *International Journal of Pharmaceutics*, *256*(1–2), 25–32. http://doi.org/10.1016/S0378-5173(03)00059-0

Gombás Á., Szabó-Révész P., Kata M. Regdon G., & Eros I. (2002). Quantitative determination of crystallinity of ??-lactose monohydrate by DSC. *Journal of Thermal Analysis and Calorimetry*, *68*(2), 503–510. http://doi.org/10.1023/A:1016039819247

Grasmeijer F., Lexmond A. J., Van Den Noort M., Hagedoorn P., Hickey, A. J., Frijlink, H. W., & De Boer, A. H. (2014). New mechanisms to explain the effects of added lactose fines on the dispersion performance of adhesive mixtures for inhalation. *PLoS ONE*, *9*(1), 1–11. http://doi.org/10.1371/journal.pone.0087825

Groneberf D. A., Witt C., Wagner U., Chung K. F., & Fischer A. (2003). Fundamentals of pulmonary drug delivery. *Respiratory Medicine*, *97*(4), 382–387. http://doi.org/10.1053/rmed.2002.1457

Haque K. (2005). Crystallization and X-ray diffraction of spray-dried and freeze-dried amorphous lactose, *340*, 293–301. http://doi.org/10.1016/j.carres.2004.11.026

Hickey A. J., Durham P. G., Dharmadhikari A., & Nardell E. A. (2015). Inhaled drug treatment for tuberculosis: Past progress and future prospects. *Journal of Controlled Release : Official Journal of the Controlled Release Society*, *240*, 127–134. http://doi.org/10.1016/j.jconrel.2015.11.018

Hickey A. J., Mansour H. M., Telko M. J., Xu Z., Smyth H. D. C., Mulder,T., … Papadopoulos D. (2007). Physical characterization of component particles included in dry powder inhalers. I. Strategy review and static characteristics. *Journal of Pharmaceutical Sciences*, *96*(5), 1282–1301. http://doi.org/10.1002/jps.20916

Hooton J. C., Jones M. D., & Price R. (2006). Predicting the behavior of novel sugar carriers for dry powder inhaler formulations via the use of a cohesive–adhesive force balance approach. *Journal of Pharmaceutical Sciences*, *95*(6), 1288–1297. http://doi.org/10.1002/jps.20618

Hoppentocht M., Hagedoorn P., Frijlink H. W., & de Boer A. H. (2014). Technological and practical challenges of dry powder inhalers and formulations. *Advanced Drug Delivery Reviews*, *75*, 18–31. http://doi.org/10.1016/j.addr.2014.04.004

Islam N., & Gladki E. (2008). Dry powder inhalers (DPIs)—A review of device reliability and

innovation. *International Journal of Pharmaceutics*, *360*(1), 1–11. http://doi.org/10.1016/j.ijpharm.2008.04.044

Jawad R., Elleman C., Vermeer L., Drake A. F., Woodhead B., Martin G. P., & Royall P. G. (2012). The measurement of the β/α anomer composition within amorphous lactose prepared by spray and freeze drying using a simple 1H-NMR method. *Pharmaceutical Research*, *29*(2), 511–524. http://doi.org/10.1007/s11095-011-0575-6

Jones M. D., Santo J. G. F., Yakub B., Dennison M., Master H., & Buckton G. (2010). The relationship between drug concentration, mixing time, blending order and ternary dry powder inhalation performance. *International Journal of Pharmaceutics*, *391*(1–2), 137–147. http://doi.org/10.1016/j.ijpharm.2010.02.031

Jones M. D., Young P., & Traini D. (2012). The use of inverse gas chromatography for the study of lactose and pharmaceutical materials used in dry powder inhalers ☆. *Advanced Drug Delivery Reviews*, *64*(3), 285–293. http://doi.org/10.1016/j.addr.2011.12.015

Kawashima Y., Serigano T., Hino T., Yamamoto H., & Takeuchi H. (n.d.). Effect of surface morphology of carrier lactose on dry powder inhalation property of pranlukast hydrate. *International Journal of Pharmaceutics*, *172*(1–2), 179–188. Retrieved from http://cat.inist.fr/?aModele=afficheN&cpsidt=1603199

Kinnunen H., Hebbink G., Peters H., Huck D., Makein L., & Price R. (2015). Extrinsic lactose fines improve dry powder inhaler formulation performance of a cohesive batch of budesonide via agglomerate formation and consequential co-deposition. *International Journal of Pharmaceutics*, *478*(1), 53–59. http://doi.org/10.1016/j.ijpharm.2014.11.019

Kirch J., Schneider A., Abou B., Hopf A., Schaefer U. F., Schneider M., … Lehr C.-M. (2012). Optical tweezers reveal relationship between microstructure and nanoparticle penetration of pulmonary mucus. *Proceedings of the National Academy of Sciences of the United States of America*, *109*(45), 18355–60. http://doi.org/10.1073/pnas.1214066109

Kirk J. H., Dann S. E., & Blatchford C. G. (2007). Lactose: A definitive guide to polymorph determination. *International Journal of Pharmaceutics*, *334*(1–2), 103–114. http://doi.org/10.1016/j.ijpharm.2006.10.026

Kleinstreuer C., Zhang Z., & Donohue J. F. (2008). Targeted drug-aerosol delivery in the human respiratory system. *Annual Review of Biomedical Engineering*, *10*, 195–220. http://doi.org/10.1146/annurev.bioeng.10.061807.160544

Le V. N. P., Robins E., & Flament M. P. (2010). Air permeability of powder: A potential tool for Dry Powder Inhaler formulation development. *European Journal of Pharmaceutics and Biopharmaceutics*, *76*(3), 464–469. http://doi.org/10.1016/j.ejpb.2010.09.003

Lehto V., Tenho M., Vähä-heikkilä K., & Harjunen P. (2006). The comparison of seven different methods to quantify the amorphous content of spray dried lactose, *167*, 85–93. http://doi.org/10.1016/j.powtec.2006.05.019

Lippmann. (1976). Deposition, retention, and clearance of inhaled particles. In *Environmental Health Perspectives* (Vol. Vol.16, pp. 41–53). http://doi.org/http://dx.doi.org/10.1016/B978-012352335-8/50089-2

Listiohadi Y., & Hourigan J. (2009). Thermal analysis of amorphous lactose and alpha-lactose monohydrate. *Dairy Science and …*, *89*, 43–67. http://doi.org/10.1051/dst:2008027

Louey M. D., & Stewart P. J. (2002). Particle interactions involved in aerosol dispersion of ternary interactive mixtures. *Pharmaceutical Research*, *19*(10), 1524–1531. http://doi.org/10.1023/A:1020464801786

Lucas P., Anderson K. & Staniforth J. N. (1998). Protein Deposition from Dry Powder Inhalers: Fine Particle Multiplets as Performance Modifiers. Retrieved from http://link.springer.com/article/10.1023/A:1011977826711

Pilcer G., Wauthoz N., & Amighi K. (2012). Lactose characteristics and the generation of the aerosol. *Advanced Drug Delivery Reviews*, *64*(3), 233–256.

http://doi.org/10.1016/j.addr.2011.05.003

Podczech F. (1998). The relationship between physical properties of lactose monohydrate and the aerodynamic behaviour of adhered drug particles. *International Journal of Pharmaceutics*, *160*(1), 119–130. Retrieved from http://cat.inist.fr/?aModele=afficheN&cpsidt=2132612

Podczeck F. (1998). Evaluation of the Adhesion Properties of Salbutamol Sulphate to Inhaler Materials. *Pharmaceutical Research*, *Volume 15*(Issue 5), pp 806–808. http://doi.org/10.1023/A:1011947809390

Ramé E. (1997). The Interpretation of Dynamic Contact Angles Measured by the Wilhelmy Plate Method. *Journal of Colloid and Interface Science*, *185*(1), 245–251. http://doi.org/10.1006/jcis.1996.4589

Saleem I., Smyth H., & Telko M. (2008). Prediction of dry powder inhaler formulation performance from surface energetics and blending dynamics. *Drug Development and Industrial Pharmacy*, *34*(November), 1002–1010. http://doi.org/10.1080/03639040802154905

Schrader M. E. (1995). Young-Dupre Revisited. *Langmuir*, *11*(9), 3585–3589. http://doi.org/10.1021/la00009a049

Shur J., Harris H., Jones M. D., Kaerger J. S., & Price R. (2008). The role of fines in the modification of the fluidization and dispersion mechanism within dry powder inhaler formulations. *Pharmaceutical Research*, *25*(7), 1631–1640. http://doi.org/10.1007/s11095-008-9538-y

Singh D. J., Jain R. R., Soni P. S., Abdul S., Darshana H., Gaikwad R. V, & Menon M. D. (2014). Preparation and Evaluation of Surface Modified Lactose Particles for Improved Performance of Fluticasone Propionate Dry Powder Inhaler. *Journal of Aerosol Medicine and Pulmonary Drug Delivery*, *28*(4), 254–267. http://doi.org/10.1089/jamp.2014.1146

Steckel H., & Bolzen N. (2004). Alternative sugars as potential carriers for dry powder inhalations. *International Journal of Pharmaceutics*, *270*(1–2), 297–306. http://doi.org/10.1016/j.ijpharm.2003.10.039

Stuart B. O. (1999). 14 - Deposition and Clearance of Inhaled Particles, *55*, 295–324. http://doi.org/http://dx.doi.org/10.1016/B978-012352335-8/50089-2

Tay T., Das S., & Stewart P. (2010). Magnesium stearate increases salbutamol sulphate dispersion: What is the mechanism? *International Journal of Pharmaceutics*, *383*(1–2), 62–69. http://doi.org/10.1016/j.ijpharm.2009.09.006

Telko M. J., & Hickey A. J. (2005). Dry powder inhaler formulation. *Respiratory Care*, *50*(9), 1209–1227. http://doi.org/10.2165/00128413-200615470-00016

Van Oss C. J., Chaudhury M. K., & Good R. J. (1988). Interfacial Lifshitz-van der Waals and polar interactions in macroscopic systems. *Chemical Reviews*, *88*(6), 927–941. http://doi.org/10.1021/cr00088a006

Van Oss C. J., Giese R. F., & Wu W. (1997). On the predominant electron-donicity of polar solid surfaces. *Journal of Adhesion*, *63*(1–3), 71–88. http://doi.org/10.1080/00218469708015214

Watling C. P., Elliott J. A., & Cameron R. E. (2010). Entrainment of lactose inhalation powders: A study using laser diffraction. *European Journal of Pharmaceutical Sciences*, *40*(4), 352–358. http://doi.org/10.1016/j.ejps.2010.04.009

Weibel E. R., Sapoval B., & Filoche M. (2005). Design of peripheral airways for efficient gas exchange. *Respiratory Physiology and Neurobiology*, *148*(1–2 SPEC. ISS.), 3–21. http://doi.org/10.1016/j.resp.2005.03.005

Williams R. O., Carvalho T. C., & Peters J. I. (2011). Influence of particle size on regional lung deposition - What evidence is there? *International Journal of Pharmaceutics*, *406*(1–2), 1–10. http://doi.org/10.1016/j.ijpharm.2010.12.040

Young P. M., Cocconi D., Colombo P., Bettini R., Price R., Steele D. F., & Tobyn M. J. (2002). Characterization of a surface modified dry powder inhalation carrier prepared by "particle smoothing". *The Journal of Pharmacy and Pharmacology*, *54*, 1339–1344. http://doi.org/10.1211/002235702760345400

Zeng X. M., Martin G. P., Tee S. K., Ghoush A. A., & Marriott C. (1999). Effects of particle size and adding sequence of fine lactose on the deposition of salbutamol sulphate from a dry powder formulation. *International Journal of Pharmaceutics*, *182*(2), 133–144. http://doi.org/10.1016/S0378-5173(99)00021-6

Zeng X. M., Martin G. P., Tee S. K., & Marriott C. (1998). The role of fine particle lactose on the dispersion and deaggregation of salbutamol sulphate in an air stream in vitro. *International Journal of Pharmaceutics*, *176*(1), 99–110. http://doi.org/10.1016/S0378-5173(98)00300-7

Zeng X., Martin G. P., Marriott C., & Pritchard J. (2001). Lactose as a carrier in dry powder formulations: The influence of surface characteristics on drug delivery. *Journal of Pharmaceutical Sciences*, *90*(9), 1424–1434. http://doi.org/10.1002/jps.1094